Proliferating activity in a bryozoan lophophore

Natalia Shunatova [Corresp., 1] , Ilya Borisenko [2]

1 Department of Invertebrate Zoology, Biological Faculty, St. Petersburg State University, St. Petersburg, Russia

2 Department of Embryology, Biological Faculty, St. Petersburg State University, St. Petersburg, Russia

Corresponding Author: Natalia Shunatova
Email address: n.shunatova@spbu.ru

Bryozoans are small benthic colonial animals; their colonies consist of zooids which are composed of a cystid and polypide. According to morphological and molecular data, three classes of bryozoans are recognized: Phylactolaemata, Gymnolaemata and Stenolaemata. Bryozoans are active suspension feeders and their feeding apparatus, the lophophore, is fringed with a single row of ciliated tentacles. In gymnolaemates, the lophophore is bell-shaped and its tentacles may be equal in length (equitentacled lophophores) or some tentacles may be longer than others (obliquely truncated lophophores). In encrusting colonies, polypides with obliquely truncated lophophores usually border specific sites of excurrent water outlets (colony periphery and chimneys) where depleted water has to be removed. It is known that during colony astogeny, colony-wide water currents rearrange: new chimneys are formed and/or location of the chimneys within a given colony changes with time. Such rearrangement requires remodeling of the lophophore shape and lengthening of some tentacles in polypides surrounding water outlets. However, proliferating activity has not been described for bryozoans. Here, we compared the distribution of S-phase and mitotic cells in young and adult polypides in three species of Gymnolaemata. We tested the hypothesis that tentacle growth/elongation is intercalary and cell proliferation takes place somewhere at the lophophore base because such pattern does not interfere with the feeding process. We also present a detailed description of ultrastructure of two parts of the lophophore base: the oral region and ciliated pits, and uncover the possible function of the latter. Presence of stem cells within the ciliated pits and the oral region of polypides provide evidence that both sites participate in tentacle elongation. This confirms the suggested hypothesis about intercalary tentacle growth which provides a potential to alter a lophophore shape in adult polypides according to rearrangement of colony wide water currents during colony astogeny. For the first time deuterosome-like structures were revealed during kinetosome biogenesis in the prospective multiciliated epithelial cells in invertebrates. Tentacle regeneration experiments in Electra pilosa demonstrated that among all epidermal cell types, only non-

ciliated cells at the abfrontal tentacle surface are responsible for wound healing. Ciliated cells on the frontal and lateral tentacle surfaces are specialized and unable to proliferate, not even under wound healing. Tentacle regeneration in *E.pilosa* is very slow and similar to the morphallaxis type. We suggest that damaged tentacles recover their length by a mechanism similar to normal growth, powered by proliferation of cells both within ciliated pits and the oral region.

1 **Proliferating activity in a bryozoan lophophore**

3 Natalia Shunatova[1] and Ilya Borisenko[2]
4 [1] – Department of Invertebrate Zoology, Biological Faculty, St. Petersburg State University,
5 Universitetskaya nab., 7/9, St. Petersburg 199034, Russian Federation.
6 [2] – Department of Embryology, Biological Faculty, St. Petersburg State University,
7 Universitetskaya nab., 7/9, St. Petersburg 199034, Russian Federation.
8 Corresponding author:
9 Natalia Shunatova[1]
10 Department of Invertebrate Zoology, St. Petersburg State University, Universitetskaya nab., 7/9,
11 St. Petersburg 199034, Russian Federation.
12 Email address: n.shunatova@spbu.ru, natalia.shunatova@gmail.com

Abstract

15 Bryozoans are small benthic colonial animals; their colonies consist of zooids which are
16 composed of a cystid and polypide. According to morphological and molecular data, three
17 classes of bryozoans are recognized: Phylactolaemata, Gymnolaemata and Stenolaemata.
18 Bryozoans are active suspension feeders and their feeding apparatus, the lophophore, is fringed
19 with a single row of ciliated tentacles. In gymnolaemates, the lophophore is bell-shaped and its
20 tentacles may be equal in length (equitentacled lophophores) or some tentacles may be longer
21 than others (obliquely truncated lophophores). In encrusting colonies, polypides with obliquely
22 truncated lophophores usually border specific sites of excurrent water outlets (colony periphery
23 and chimneys) where depleted water has to be removed. It is known that during colony astogeny,
24 colony-wide water currents rearrange: new chimneys are formed and/or location of the chimneys
25 within a given colony changes with time. Such rearrangement requires remodeling of the
26 lophophore shape and lengthening of some tentacles in polypides surrounding water outlets.
27 However, proliferating activity has not been described for bryozoans. Here, we compared the
28 distribution of S-phase and mitotic cells in young and adult polypides in three species of
29 Gymnolaemata. We tested the hypothesis that tentacle growth/elongation is intercalary and cell
30 proliferation takes place somewhere at the lophophore base because such pattern does not
31 interfere with the feeding process. We also present a detailed description of ultrastructure of two
32 parts of the lophophore base: the oral region and ciliated pits, and uncover the possible function
33 of the latter. Presence of stem cells within the ciliated pits and the oral region of polypides
34 provide evidence that both sites participate in tentacle elongation. This confirms the suggested
35 hypothesis about intercalary tentacle growth which provides a potential to alter a lophophore
36 shape in adult polypides according to rearrangement of colony wide water currents during colony
37 astogeny. For the first time deuterosome-like structures were revealed during kinetosome
38 biogenesis in the prospective multiciliated epithelial cells in invertebrates. Tentacle regeneration
39 experiments in *Electra pilosa* demonstrated that among all epidermal cell types, only non-
40 ciliated cells at the abfrontal tentacle surface are responsible for wound healing. Ciliated cells on
41 the frontal and lateral tentacle surfaces are specialized and unable to proliferate, not even under
42 wound healing. Tentacle regeneration in *E.pilosa* is very slow and similar to the morphallaxis
43 type. We suggest that damaged tentacles recover their length by a mechanism similar to normal
44 growth, powered by proliferation of cells both within ciliated pits and the oral region.

45

Introduction

46

47   Cell proliferation is the main contributor to the growth of an organism and also participates
48   in maintenance of its body during the lifespan. In adults, proliferating cells contribute to
49   physiological cell turnover and replacement of injured cells and tissues. Different aspects of cell
50   proliferation during morphogenesis and regeneration were described for various animals:
51   sponges (e.g., Alexander et al., 2014; Borisenko et al., 2015; Ereskovsky et al., 2015; Kahn &
52   Leys, 2016), cnidarians (e.g., Chera et al., 2009; Fritz et al., 2013; Gahan et al., 2016),
53   plathyhelminths (e.g., Reddien & Sánchez Alvarado, 2004; Salo et al., 2009; Cebrià, Adell &
54   Saló, 2018), annelids (e.g., Fischer & Dorresteijn, 2004; Paulus & Müller, 2006; Birkmann &
55   Wanninger, 2010; Gridza, 2010; Yoshida-Noro & Tochinai, 2010; Bely, 2014), insects (e.g.,
56   Milán, Campuzano & García-Bellido, 1996; Neufeld et al., 1998; Baonza & Freeman, 2005),
57   mollusks (e.g., Grimaldi et al., 2004; Henry, Okusu & Martindale, 2004; Redl et al., 2016),
58   vertebrates (e.g., Hay & Fischman, 1961; Bettencourt-Dias, Mittnacht & Brockes, 2003; Warren,
59   Puskarczyk & Chapman, 2009), etc. However, many bilaterian taxa, including bryozoans, are
60   still unexplored in this respect.
61   Bryozoans are small benthic animals which are almost exclusively colonial (Schwaha et al.,
62   2019). Their colonies consist of zooids, which are composed of a cystid (immovable part, often
63   calcified) and polypide (movable soft tissues: a lophophore, tentacle sheath, gut and associated
64   muscles, and nervous system). According to morphological and molecular data, three classes of
65   bryozoans are recognized: Phylactolaemata, Gymnolaemata and Stenolaemata (Mukai, Terakado
66   & Reed, 1997; Waeschenbach, Taylor & Littlewood, 2012). Gymnolaemates are the most
67   diverse and abundant extant bryozoan group. In all groups of bryozoans polypides are short lived
68   and degenerate after a few weeks with a formation of a residual mass, or brown body. Cystids
69   survive much longer even in Phylactolaemata: polypides in this group never regenerate. In the
70   majority of gymnolaemates and stenolaemates a polypide regenerates within the same cystid.
71   The general overview of this process was provided for several species at light microscopic level
72   (see Mukai, Terekado and Reed, 1997 for a review). Such regular degeneration-regeneration
73   cycles require the presence of stem cells within each zooid.
74   Bryozoans are active suspension feeders (Jørgensen, 1966) and their feeding apparatus, a
75   lophophore, is fringed with a single row of ciliated tentacles. Tentacle ultrastructure has been
76   described for three species of Gymnolaemata (Lutaud, 1973; Smith, 1973; Gordon, 1974; Mukai,
77   Terekado & Reed, 1997). The outer tentacle epithelium includes both non-ciliated and ciliated
78   cells; the latter are arranged in five longitudinal rows and, correspondingly, form five ciliary
79   bands: a single frontal band and paired latero-frontal and lateral bands. Functions of ciliary bands
80   are well understood: they create a water current and participate in the capture of food. The
81   tentacle epidermis rests on a thick layer of extracellular matrix (ECM), which is continuous with
82   that of the lophophore base. Each tentacle houses a coelomic cavity which is an outgrowth of the
83   lophophore coelom. The coelomic lining of the tentacles includes both epithelial cells on the
84   lateral surfaces and myoepithelial cells on the frontal and abfrontal sides. Myoepithelial cells
85   form the frontal and abfrontal tentacle muscles. Within a lophophore, tentacles may be equal in
86   length (equitentacled lophophores) or some tentacles may be longer than the other (obliquely
87   truncated lophophores).
88   The tentacles unite at their bases and join the lophophore base which is very complex in
89   structure. At this region the tentacle coeloms join the ring coelomic canal surrounding the mouth.
90   There is a single description of the microanatomy of the lophophore base in *Cryptosula*
91   *pallasiana* Moll, 1803 by Gordon (1974). He found a specific structure between tentacle bases

92 and termed them 'ciliated pits'. The ciliated pits are small structures (about 3 μm in diameter and
93 25-30 μm deep), and their upper two thirds are ciliated. A similar structure was reported by
94 Schwaha and Wood (2011) for a ctenostome *Hislopia malayensis* Annandale, 1916.
95 Unfortunately, in both cases the authors provided no further details on their structure and
96 mentioned that the possible function of the ciliated pits is unknown.
97   During feeding, the tentacle ciliation is responsible for creating water currents bringing
98 food to the lophophore and participates in particle retention and transport. Food-depleted water
99 leaves the lophophore between the tentacles and has to be removed from the colony. Different
100 variants of colony-wide water currents were described for bryozoans. Among them, the most
101 specific way of the water removal in encrusting colonies is a formation of excurrent water
102 outlets, or chimneys, which were first described for large colonies of *Membranipora*
103 *membranacea* Linnaeus, 1767 (Banta, McKinney & Zimmer, 1974). Several types of chimneys
104 are recognized, and there is a vast literature describing them. In many cases, the chimneys are
105 surrounded by the polypides with obliquely truncated lophophores, and their longest tentacles
106 border the chimney (e.g., Cook, 1977; Winston, 1978, 1979; Cook & Chimonides, 1980;
107 Lidgard, 1981; Dick, 1987; McKinney, 1990). The rest of the polypides in the colony usually
108 have equitentacled lophophores. Polypides with obliquely truncated lophophores are also located
109 at the colony periphery, and their longest tentacles face the colony edge. During colony
110 astogeny, either new chimneys are formed, and/or the location of the chimneys within the given
111 colony changes with time (von Dassow, 2005a, b, 2006). In many cases, this happens during the
112 same degeneration-regeneration cycle. Thus, the question arises: are the polypides surrounding
113 the new chimney capable of lengthening some of their tentacles and changing the shape of their
114 lophophores? For two cheilostomes *Holoporella brunnea* [=*Celleporaria brunnea* Hincks, 1884]
115 and *Membranipora serrilamella* [=*M. villosa* Hincks, 1880], Dick (1987) mentioned the
116 possibility of a transformation from obliquely truncated lophophore to equitentacled one, and
117 vice versa. He suggested that the reason for this transformation is the lophophore position
118 respective to the changing excurrent flow.
119   Considering data reported by Dick (1987), one can suggest that such an elongation of the
120 tentacles implies the presence of proliferating cells either in the tentacle itself or at the
121 lophophore base. Proliferating activity within the lophophore has not been described for
122 bryozoans. Nevertheless, the presence of blastemic cells was mentioned within the oral region of
123 the polypide in *C. pallasiana* (Gordon, 1974) and close to the ganglion of a degenerating female
124 polypide in *Alcyonidium polyoum* Hassall, 1841 (Matricon, 1963).
125   It is well known that different benthic animals prey on bryozoans using different
126 mechanisms, and usually they consume a whole polypide or a considerable part of it (Iyengar
127 &Harvell, 2002; Berning, 2007; Lidgard, 2008; Lindsay, 2010). However, there is a single report
128 that individual tentacles could be bitten off by a predator: Marcus (1941) described that
129 chironomid larvae bite off the tips of tentacles in polypides of the genus *Stolella*
130 (Phylactolaemata). He also pointed out that such bitten tentacles regenerate. The experimental
131 regeneration of tentacles was studied only in phylactolaemates, and it was demonstrated that
132 tentacles, when cut off, regenerate in the course of several days (Otto, 1921; Oda, 1954).
133 Unfortunately, both authors did not provide any data on the location of proliferating cells.
134 Similar data on gymnolaemates and stenolaemates are absent. Nevertheless, based on the idea
135 that tentacles can lengthen in adult polypides, it can be assumed that polypides have the ability to
136 regenerate damaged tentacles.

137   Here we applied EdU-labeling technique to bryozoans to study proliferating activity within
138 the lophophore. For three species of gymnolaemates with obliquely truncated lophophores, we
139 tested the hypothesis that the tentacle growth/elongation is intercalary or, in other words,
140 proliferating cells are not scattered along the tentacle but are located in a specific site(s) within
141 the lophophore base. Such pattern makes the tentacle elongation possible without interfering
142 with the feeding process. We present a detailed description of two regions of the lophophore base
143 housing proliferating cells: the oral region and ciliated pits in four gymnolaemate species. We
144 also tried to detect the regenerative capacity of polypides in *Electra pilosa* Linnaeus, 1767 after
145 microsurgical amputation of the distal part of the tentacles.
146

Material and methods

148 **Animals**
149   We studied fine structure of the lophophore base in four species: *Rhamphostomella ovata*
150 Smitt, 1868; *Electra pilosa* Linnaeus, 1767; *Aquiloniella scabra* van Beneden, 1848, and
151 *Eucratea loricata* Linnaeus, 1758 (Gymnolaemata: Cheilostomatida). Proliferating activity was
152 registered in *R. ovata*, *E. pilosa*, and *A. scabra*: these species have both equitentacles and
153 obliquely truncated lophophores. Material was collected in the vicinity of Research and
154 Educational Station "Belomorskaya" of SPbSU (White Sea, Kandalaksha Bay, Chupa Inlet) by
155 SCUBA diving in 2016-2017.
156   *R. ovata* and *E. pilosa* have encrusting colonies with centrifugal growth, and the youngest
157 zooids are located at the colony periphery. *A. scabra* and *E. loricata* have erect colonies with
158 youngest zooids located at the tips of the branches.
159   Different age classes of zooids were referred as followed. The youngest zooids with fully
160 developed and feeding polypides, which are the closest to the growth margin, are assigned as the
161 1st age class. Zooids of the 1st age class were budded by the zooids of the 2nd age class; zooids of
162 the 2nd age class were budded by zooids of the 3rd age class, etc. Polypides of the 1st and 2nd age
163 classes are referred here as 'young' polypides, and polypides of 4th and older age classes as
164 'adult' polypides.
165 **Transmission electron microscopy (TEM) and scanning electron microscopy (SEM) study**
166   Ten colonies of each species were anesthetized in the mixture of isotonic solution of
167 magnesium chloride and seawater (ratio 1:1) and fixed in 2.5% glutaraldehyde solution in 0.1 M
168 isotonic cacodylate buffer (supplemented with sucrose to reach 750 mOsmol). For TEM five
169 colonies of each species were postfixed with 1% osmium tetroxide in 0.1 M cacodylate buffer
170 (supplemented with sucrose to reach 750 mOsmol), dehydrated through a graded ethanol series,
171 transferred through an ethanol–acetone mixture to pure acetone and then embedded in epoxy
172 resin. Serial sections were obtained on an ultramicrotome Leica EM UC7 using diamond knife in
173 different projections. Semithin sections were stained with toluidine blue; ultrathin sections were
174 stained in uranyl acetate and lead citrate and then investigated with Jeol JEM 1400 electron
175 microscope. For SEM five colonies of each species were processed according to standard
176 protocols, critical point dried, and sputter coated with 20 nm gold. Scanning electron
177 micrographs were made using a Tescan MIRA3 LMU electron microscope. The images were
178 processed with Photoshop CS5.
179 **Proliferating activity**
180   Proliferating activity was detected by incorporation of labeled thymidine analog, 5-ethynyl-
181 2'-deoxyuridine (or EdU), during S-phase of cell cycle, with subsequent visualization of labeled

182   DNA by click-reaction (Salic and Mitchinson, 2008). EdU and the reactive dye, sulfo-Cyanine5
183   azide, were obtained from Lumiprobe (Russia). Five colonies of each species were placed in
184   filtered sea water with 100 or 300 μM EdU, diluted from 250 mM stock in DMSO. Animals
185   were incubated during 3 and 6 hours at 7°C in Petri dishes. After that, colonies were anesthetized
186   as described above and fixed in 4% PFA in 0.1 M PBS (pH 7.4) overnight. Some polypides
187   remained retracted during anesthetization; in such cases we dissolved a calcified layer of
188   ectocyst with 5% EDTA in 0.1M PBS before staining. Fixed colonies were washed in 0.1M PBS
189   with addition of 0.1% Tween-20 three times (10 min each) and permeabilized with 0.5% Triton
190   X-100 in 0.1M PBS during 15 min on a shaker. After rinsing in PBS, colonies were incubated in
191   staining mix (Tris-HCl pH 8.5 100 mM, $CuSO_4$ 4 mM, sulfo-Cyanine5 azide 2 μM, ascorbic acid
192   50 mM) during 1 h at room temperature in the dark. Then colonies were rinsed 0.1M PBS with
193   addition of 0.1% Tween-20 two times (10 min each) and blocked in 5% sheep serum in 0.1M
194   PBS with addition of 0.1% Tween-20 during 1 h on a shaker. Nuclei were counterstained with
195   DAPI at 1 μg/ml. Polypides were extracted with fine needles under stereomicroscope and
196   mounted in glycerol with DABCO addition as an antifade. Specimens were examined using the
197   confocal laser scanning microscope Leica TCS SPE. The images were processed by ImageJ
198   software (FiJi).

199   **Regeneration experiments**
200   Regeneration experiments were made only for *Electra pilosa*. The most probable damage
201   not followed by zooid death is biting off the distal part of tentacle(s) by a predator. We chose 10
202   large colonies including about 350-400 zooids and anesthetized them (as described above). In
203   each colony we selected 10 polypides belonging to the 5th and 6th age classes and amputated the
204   distal part (from ¼ to ½) of 2-4 tentacles. After that, colonies were washed in seawater to remove
205   anesthetic and were kept in seawater in isothermic room at 7°C. Colonies were fixed after 24, 48,
206   72, 120 and 148 hours (two colonies each time), and six hours prior fixation colonies were
207   moved to the mixture of EdU (final concentration of 300 μM) and isotonic solution of
208   magnesium chloride. After labeling, colonies were fixed in 4% PFA in 0.1M PBS and processed
209   as described above.

210

211   # Results

212   **General remarks on tentacle structure**
213   Polypides of studied species possess different number of tentacles: 10 in *Eucratea loricata*,
214   12-16 in *Electra pilosa*, 14-17 in *Rhamphostomella ovata* and *Aquiloniella scabra*. General view
215   of feeding polypides is given in Fig. 1A. In all studied species, the tentacles are covered with a
216   one-layered epithelium; its cells are arranged in nine continuous and one (the tenth) intermittent
217   rows (Fig. 1B). Following Smith (1973), we used an alphabetical code to refer to the different
218   cell types (Fig. 1C). The frontal side of the tentacle is covered with a single row of A-cells
219   (frontal cells). Paired rows of latero-frontal B-cells are located on either side of the frontal A-
220   cells. Paired fronto-lateral (C-cells) and abfronto-lateral (D-cells) rows cover the lateral surfaces
221   of the tentacle. The abfrontal surface of the tentacle is composed of paired rows of abfrontal E-
222   cells. Between them, at the midline of the abfrontal surface, there is a single intermittent row of
223   F-cells.
224   Each tentacle possesses five longitudinal ciliary bands described for Bryozoa. The frontal
225   band is formed by cilia of multiciliated A-cells, the latero-frontal bands are composed of cilia of
226   monociliated B-cells, and the lateral bands includes cilia of multiciliated C- and D-cells (Fig.

227   1D). The abfrontal tentacle surface bears regularly alternated multi- and monociliated putative
228   sensory F-cells (Fig. 2A), and each tentacle tip has a terminal tuft of several cilia belonging to 3
229   – 4 apical cells. The alternating arrangement of mono- and multiciliated F-cells was similar to
230   that described before (see Shunatova & Nielsen, 2002). Thus, in 'adult' polypides of all studied
231   species, both mono- and multiciliated F-cells were more or less evenly spaced along the entire
232   tentacle length, with an average distance between them of about 10-15 μm (Figs. 2A–2B).
233   However, at the tentacle bases of young polypides (1st and 2nd age classes), the distance between
234   F-cells is much shorter than that in the distal and middle parts of the same tentacle (Fig. 2C).
235   The tentacle epithelium is supported with a prominent ECM layer which forms a hollow
236   tube with two longitudinal abfronto-lateral ridges, or horns. Fine structure of the cells of the
237   tentacle coelomic lining has been recently described in details (see Shunatova &Tamberg, 2019).
238   Along the entire tentacle length, cell composition of tentacles in studied species is identical.

239 **Lophopore base**

240   Lophophore base is very complex in structure and here we address only two sites: ciliated
241   pits and the region surrounding the mouth. The structure of each region is the same in young and
242   adult polypides (except for the number of the cells undergoing mitosis – see below).

243 *Ciliated pits*

244   At the proximal end of the tentacle, the number of E-cells increases from two to three, and
245   they combine both with the E-cells of the adjoining tentacles and with the epidermis of the
246   tentacle sheath (Figs. 3A–3B). At this level, the abfronto-lateral horns of the tentacle ECM
247   change their shape: it becomes irregular conical in cross sections. Between them, two additional
248   small projections of the tentacle ECM appear; they are located between the bases of E-cells
249   (Figs. 3A–3B). Each of the four projections gives rise to a thin outgrowth of ECM, and together
250   they envelope the basal portions of E-cells and combine with the ECM of the tentacle sheath
251   (Figs. 3B–3C). These outgrowths also stretch basally and unite with the ECM of the septum
252   dividing the lophophore and main body cavity (Fig. 3C). At this level, B- and C-cells of adjacent
253   tentacles contact each other (Fig. 3D) and isolate the lumen of the ciliated pit.

254   The ciliated pits are blind-ended conical invaginations of the epidermis between the
255   tentacle bases (Figs. 3E–3F). The number of the ciliated pits corresponds to the tentacle number.
256   The opening of the ciliated pit is surrounded with C- and D-cells of adjacent tentacles and a
257   single E-cell which shifted from either of the tentacles; the latter takes the abfrontal side of the
258   ciliated pit. Basally, these five cells are followed by five vertical cell rows composing the walls
259   of the ciliated pit, and here we use the following designation for them. Rows of CP- and DP-cells
260   are located below the corresponding C- and D-cells of the neighboring tentacles and a single row
261   of EP-cells occupies the abfrontal surface of the ciliated pit (Fig. 4). The depth of the ciliated pits
262   varies across studied species. The deepest ciliated pits were found in *R. ovata* (about 30 μm):
263   they include up to 11 cells in the CP- and DP-rows and up to 7 cells in the EP-row. Polypides of
264   *E. loricata* have the shortest ciliated pits (about 10 μm): their CP- and DP-rows are composed of
265   3 cells, and EP-row includes only two cells. Three regions are recognized along the axis of the
266   ciliated pit: distal, middle and proximal (Figs. 3F and 4).

267   The distal part of the ciliated pit houses a prominent funnel-shaped lumen that opens into
268   the environment. The fine structure of both CP- and DP-cells in general resembles that of C- and
269   D-cells, although the shape of the cells change to an irregular trapezoid and their apical surface is
270   limited by the lumen of the ciliated pit (Figs. 5A–5B). The number of cilia decreases towards the
271   middle region of the ciliated pit and the regularity of their arrangement is lost (Fig. 5C). Each
272   cilium of CP- and DP-cells possesses a single kinetosome with two cross-striated rootlets

273 resembling that of cilia in C- and D-cells in location though lateral rootlets in CP-cells are rather
274 short (Figs. 5A–5B). Non-ciliated EP-cells are trapezoid in shape with irregularly shaped nuclei
275 and the usual set of organelles (Fig. 5D). The area of the apical surface of each cell type
276 decreases towards the bottom of the ciliated pit.
277   The middle part of the ciliated pit contains a very narrow tube-shaped lumen; usually there
278 is a single cilium within it (Fig. 6A), and only two out of the ciliated pits lack cilia. This cilium
279 arises from the CP-cell located at the bottom of the lumen; the rest of CP- and DP-cells in the
280 middle part are non-ciliated. Sometimes, the uppermost CP- and DP-cells in this region (i.e.
281 located at the border with the distal part of the ciliated pit) possess numerous irregularly arranged
282 kinetosomes located within the apical part of the cells (Fig. 6B). Some CP- and DP-cells, located
283 more basally, demonstrate different stages of kinetosome biogenesis. We found clusters of
284 electron-dense 'fibrogranular material' (Fig. 6C), vacuoles with fibrillar electron-dense or
285 electron-lucent content (Fig. 6D), electron-dense spherical bodies (or deuterosome-like
286 structures) surrounded with numerous procentrioles (Figs. 6A, 6C and 6E). Often, one of the
287 procentrioles is larger and lies at the right angle to the others (Fig. 6e). Rarely, the named stages
288 are present simultaneously in the same cell. In all cases two to three dictyosomes of Golgi
289 complex are located close to them (Figs. 6B and 6E). At the latest stage of kinetosome
290 biogenesis, they become separated from deuterosome-like structures (Fig. 6F), and in the apical
291 part of the cells there are developing cross-striated rootlets surrounded by electron-dense
292 'fibrogranular material' (Fig. 6E).
293   The proximal region of the ciliated pit lacks a lumen and the regularity of cell arrangement
294 is lost (Fig. 7A); we denote the cells within this part as P-cells. P-cells are small, irregular- or
295 rounded in shape; they have relatively large nuclei, few mitochondria, scarce small cisterns of
296 ER, free ribosomes and rarely free kinetosomes (Figs. 7B–7C). Some P-cells undergo mitosis
297 (Figs. 7D–7E).
298 *Oral region*
299   In the most proximal part of the tentacle, the frontal row of A-cells is two cells wide (Fig.
300 8A). At the level of the openings of the ciliated pits, where C- and D-cells of adjoining tentacles
301 combine, the rows of A-, B- and C-cells join the oral region (Fig. 8B). Cells forming the outer
302 rim of the oral region lack cilia (Figs. 8C–8D), although frontal cilia often mask it (Fig. 8B). In
303 *E. loricata*, the apical surface of these cells has very long microvilli (Fig. 8D). The rest of the
304 oral region is densely ciliated. The height of the cells of the oral region gradually increases
305 towards the mouth. In *A. scabra*, *E. pilosa*, and *E. loricata* all cells of the oral region are
306 multiciliated and similar in structure. They are column-shaped with elongated or irregular shaped
307 nuclei; their cytoplasm contains numerous small membrane-bounded vesicles with electron-
308 lucent content (Fig. 8E). Each cilium has a kinetosome with two cross-striated rootlets.
309   In *R. ovata*, the peripheral part of the oral region (situated close to the outer rim at the level
310 of the middle region of the ciliated pits) is composed of two cell types. Cells located in the
311 continuation of the rows of A-cells have an electron-dense cytoplasm, and their apical surface is
312 entirely occupied by numerous cilia (Figs. 9A–9B). Between these clusters, there are cells with
313 election-gray cytoplasm. Some of them are putative secretory cells: they form small lobe-shaped
314 apical projections which are scattered between the cilia (Figs. 9B and 9D–9F). The cell
315 membrane of such projections is smooth and lacks microvilli and cuticle. It is worth noting that
316 the mouth is clogged with small drop-shaped structures with very thin and short stalk (Fig. 9C).
317 In some non-ciliated cells without apical projections, we found different stages of kinetosome
318 biogenesis: clusters of 'fibrogranular material' (Fig. 9B), deuterosome-like structures surrounded

319   with procentrioles (Fig. 9E). Few cells in this region demonstrate mitotic figures (Fig. 9F). All
320   cells located close to the mouth are multiciliated, and their structure is similar to that in other
321   studied species.

Effect of EdU concentration

323   Based on our experience with sponges, relatively high concentrations of EdU (100 and 300
324   μM) were applied to studied bryozoan species, while a suitable concentration for mammalian cell
325   culture is 10 μM (Borisenko et al., 2015; Ereskovsky et al., 2015). The fluorescence intensity of
326   nuclei labeled with 300 uM of EdU was much stronger. The labeling with 100 μM of EdU gave
327   distinguishable but weak signal, and since EdU is not as toxic as BrdU, we decided to use
328   concentration of 300 μM. We found that a three-hour incubation in EdU was not enough for
329   'adult' polypides to incorporate the label while incubation during six hours gave a stable positive
330   signal.

Proliferating activity in young and adult polypides

332   Proliferating activity in *E. pilos*a, *A. scabra*, and *R. ovata* varies depending on the age of
333   zooids: it is the highest in developing buds and gradually decreases in zooids of the older age
334   classes. In the young buds almost all nuclei are EdU-positive (Figs. 10A–10B), while different
335   parts of a given organ strongly contrast in the number of EdU-labeled cells in the late buds.
336   Thus, the distal part of the tentacles lack positive EdU signal, although many cells still
337   incorporate EdU within their proximal part (Figs. 10C–10D).

338   In the lophophore of 'young' fully developed polypides (from the 1st and 2nd age classes),
339   we detected EdU-positive signal in the lophopore base. Several EdU-positive cells are located in
340   the proximal and middle regions of the ciliated pits (Figs. 11A–11D), and a positive signal was
341   detected in CP-, DP- and EP-cells. We registered from 3 up to 16 EdU-positive cells per ciliated
342   pit. This parameter varies across ciliated pits and across polypides of the same age class for each
343   studied species (Table 1). The number of EdU-positive cells per ciliated pit was less in *E.pilosa*
344   than that in *R.ovata* and *A.scabra* (Table 1)*. Close to the outer rim of the oral region, EdU-
345   positive cells are arranged in clusters at the level of the distal and middle parts of the ciliated pits
346   (Figs. 11B and 11E). At the abfrontal tentacle surface, the EdU label was incorporated by
347   individual E-cells at the proximal end of the tentacles (Figs. 11A and 11D). In addition, in four
348   young polypides of *E. pilosa*, individual EdU-positive E-cells were also scattered within the
349   proximal part of the tentacle (Fig. 11F). In several polypides of *E. pilos*a, EdU-positive nuclei
350   were also detected in the walls of the intertentacular organ during its formation.

351   In all studied species, 'adult' polypides of the 4th and 5th age classes demonstrate EdU-
352   positive signal only in the lophophore base (except for the polypides of *E. pilosa* during the
353   formation of the intertentacular organ). Though our study is qualitative and we did not
354   statistically analyze the proliferating activity at the lophophore base, the number of EdU-positive
355   cells per the ciliated pit in 'adult' polypides is less than in 'young' ones (Table 1). A larger
356   number of EdU-positive cells in 'young' polypides probably indicates that their tentacles are still
357   lengthening until their lophophores acquire a specific shape.

Proliferating activity during tentacle regeneration

359   We traced changes in proliferating activity within the lophophores of adult polypides (5th
360   and 6th age classes) of *E. pilosa* during tentacle(s) regeneration (Fig. 12). Twenty four hours after
361   surgery, we detected a single (or rarely two) EdU-positive cell at the abfrontal tentacle surface
362   (E-cell) near wound healing. Later on, 48 h after surgery, in addition to these labeled E-cells, an
363   EdU-positive signal is detected in the cells of the tentacle coelomic lining, namely in the
364   epiperitoneal cells (Figs. 12A–D). Labeled cells of the coelomic lining were located at a distance

365   of about 50-70 μm from wound healing, as well as in the proximal part of the tentacle (Figs.
366   12C–D). EdU-positive cells were absent in the distal part of the intact tentacles. The labeling
367   pattern at the lophophore base is similar to the control zooids, although the number of EdU-
368   positive cells was greater at the base of the wounded tentacles. After 3 days (72 h after surgery),
369   the label is still present near the wound: both in the E-cells and in the cells of coelomic lining.
370   Up to 120 hours after surgery, the distribution of EdU-labeled cells remains the same (Figs. 12E–
371   G). By the 7th day of regeneration (168 h after surgery), the proliferating activity in the
372   regenerating lophophores is similar to the control ones, and the E-cells near the wound do not
373   incorporate EdU anymore. Interestingly, in one of the polypides, the label was detected in the
374   cells of the coelomic lining at the base of the wounded tentacles. The level of the EdU
375   incorporation in these nuclei is low compared with those of the epidermis of the lophophore base
376   or the epidermis of the intratentacular organ, but is clear distinguishable from the nonspecific
377   background.
378   The wounded tentacles did not restore their original length or even considerably lengthen
379   during the experiment (7 days).
380

Discussion

Ciliated pits

383   In the literature, there are only two brief mentions of ciliated (or intertentacular) pits of
384   unclear function in Gymnolaemata: in *Cryptosula pallasiana* (Gordon, 1974) and in *Hislopia*
385   *malayensis* (Schwaha & Wood, 2011). Both studies provide only a general overview, and we are
386   apparently the first to provide a detailed description of the ultrastructure of the ciliated pits in
387   cheilostomes and suggest their possible function (see below). According to our data, the
388   proximal and middle parts of the ciliated pits contain stem cells undergoing mitosis (Figs. 3F and
389   7E), and the cells within the middle part demonstrate different stages of kinetosome biogenesis
390   (Fig. 6). Though Gordon did not mention this in the text, one of his illustrations (Gordon, 1974,
391   fig. 6) demonstrates the presence of irregularly arranged kinetosomes in the apical part of one
392   cell and the mitotic figure in another. Needless to say, that our data are in a good agreement with
393   these findings. Based on this and our data on proliferating activity within the lophophore (see
394   below), we can regard the ciliated pits as a specific region providing a tentacle elongation
395   (growth) in polypides.
396   Schwaha and Wood (2011) reported that the ciliated pits in *H. malayensis* are twice as deep
397   as in *C. pallasiana*. We also detected high variability of this parameter in the studied species. It
398   is possible that the depth of ciliated pits reflects the differences in the structure of the lophophore
399   base.

Proliferating activity within the lophophore

401   The proliferating activity within the bryozoan lophophore has never been described before.
402   However, the presence of blastemic cells has been mentioned twice: in the oral region of a
403   polypide in *C. pallasiana* (Gordon, 1974) and close to the ganglion of a degenerating female
404   polypide in *Alcyonidium polyoum* (Matricon, 1963). Our data revealed the presence of stem cells
405   in the ciliated pits and in the oral region of a polypide but never in the tentacles of adult
406   polypides (Figs. 3F, 7E, 9E and 11). In addition to this, we also found different stages of
407   kinetosome biogenesis in prospective multiciliated cells undergoing specialization (Figs. 6, 9B
408   and 9E). Interestingly, even in the late buds, the EdU-label is restricted to the proximal part of
409   the tentacle and was never registered in the distal part or close to the tentacle tip. These features,

410 together with the absence of proliferating cells in the tentacles of adult polypides, demonstrate
411 the early specialization of ciliated cells and provide evidence of intercalary growth of tentacles.
412 Surprisingly, in phoronids "cells undergoing mitosis are often seen" within the tentacle
413 epidermis, "suggesting a proliferation of epidermal cells for tentacular growth and for
414 substitution of dead or damaged cells" (Pardos et al., 1991, p. 81 for both quotations).
415   According to our data, proliferating cells in the ciliated pits are the source for cells that
416 compose the lateral tentacle surfaces (C- and D-cells), while the cells of the frontal tentacle
417 surface (A- and B-cells) originate from proliferating cells of the oral region. It is very likely that
418 CP- and DP-cells give rise to C- and D-cells, respectively, since we traced the stages of
419 kinetosome biogenesis in these multiciliated cells. However, we are not so positive about the
420 source for E- and F-cells. We detected an EdU-positive signal in EP-cells and in the most basal
421 E-cells but we did not trace the fate of these labeled cells. During the tentacle growth/elongation,
422 F-cells are probably formed 'in advance' compared to E-cells, since we registered clusters of
423 tightly packed F-cells in the most basal part of the tentacle in young polypides (Fig. 2C). We did
424 not detected specific source for the cells of tentacle coelomic lining. It is probably located near
425 the proximal end of the tentacles.
426   This study revealed the possible function of the ciliated pits: it is very likely that they
427 participate in the tentacle elongation in young and adult polypides. The specific location of the
428 proliferating sites within the lophophore base provides a possibility of tentacle elongation
429 without interfering with the feeding process. Our results are in a good agreement with
430 observations made by Dick (1987) who described a transformation of obliquely truncated
431 lophophore to equitentacled one, and vice versa, for two cheilostomes *Holoporella brunnea*
432 [=*Celleporaria brunnea*] and *Membranipora serrilamella* [=*M. villosa*]. Polypides with
433 obliquely truncated lophophores usually are located at the colony periphery and also surround
434 the chimneys (excurrent water outlets within encrusting colonies – e.g., see Banta, McKinney &
435 Zimmer, 1974; Cook, 1977; Winston, 1978, 1979; Cook & Chimonides, 1980; Dick, 1987).
436 Elongated tentacles of obliquely truncated lophophores fringe the chimney area. It was
437 demonstrated that the location of the chimneys within a given colony changes with time (von
438 Dassow, 2005a, b, 2006) and an alteration of colony-wide water currents requires a remodeling
439 of the lophophore shape in the polypides surrounding the newly formed chimney. Our results
440 provide evidence for a potential altering of the lophophore shape in polypides, which is crucial
441 for encrusting colonies that need to rearrange colony-wide water currents with time.
442 **Kinetosome biogenesis**
443   The kinetosome biogenesis has been studied in great detail (both morphological and
444 molecular aspects) in different vertebrates, while similar data for invertebrates, protists and
445 plants are rather scarce. Nevertheless, several general pathways are recognized: canonical (or
446 centriolar) and non-canonical (or acentriolar, including deuterosome-mediated and several *de*
447 *novo* mechanisms) – for a review, see Nabais, Pereira & Bettencourt-Dias, 2017. Deuterosome-
448 mediated assembly of kinetosomes was first described for foetal lung in rat (Sorokin, 1968) and
449 now it has been proved to be the main pathway in different multiciliated epithelia in vertebrates
450 (Dirksen, 1991; Hagiwara, Ohwada & Takata, 2004; Al Jord et al., 2014; Balestra & Gönczy,
451 2014; Yan, Zhao & Zhu, 2016; Spassky & Meunier, 2017; Shahid & Singh, 2018). It was
452 suggested that the deuterosome-mediated pathway is specific for vertebrates (Zhao et al., 2013;
453 Nabais, Pereira & Bettencourt-Dias, 2017). It should be mentioned that for invertebrates, the
454 morphological comparison by Nabais and coauthors (Nabais, Pereira & Bettencourt-Dias, 2017)
455 was based solely on data obtained during multiciliated spermiogenesis in mollusks and insects.

456   As for multiciliated epithelial cells in invertebrates, the kinetosome formation has been
457   described only for a few species. Among them, the centriolar pathway, as a single mode for
458   kinetosome producing, was reported for prototroch cells in trochophore of *Nereis limbata* Ehlers,
459   1868 [=*Alitta succinea* Leuckart, 1847] (Kalnins, 1967). A combination of the centriolar
460   pathway and the *de novo* mechanism was reported for embryos of turbellarian *Macrostomum*
461   *hystricinum* (Tyler, 1981) and acoel *Archaphanostoma* sp. (Tyler, 1984). It was demonstrated
462   that kinetosomes are formed solely by the *de novo* mechanism in the gill filaments of scallops
463   (Ash & Stephens, 1975), the body wall of adult turbellarians (Cifrian, García-Corrales &
464   Martínez-Alos, 1992; Drobysheva, 2006, 2010), and macrocilia in ctenophores (Tamm & Tamm,
465   1988). In all described cases of the acentriolar pathway in invertebrates, specific clusters of
466   fibrous granules were present, but no structures resembling deuterosomes have ever been
467   described. In addition to these fibrous granules (or 'fibro-granular material') in bryozoans, we
468   also found that procentrioles are formed around electrone-dense spherical bodies located close to
469   the dictyosomes of Golgi complex in the apical part of the cells (Figs. 6C and 6E). These
470   spherical bodies are similar to deuterosomes described for vertebrates (e.g., Sorokin, 1968;
471   Anderson & Brenner, 1971; Dirksen, 1971, 1991; Hagiwara et al., 2000; Hagiwara, Ohwada &
472   Takata, 2004). Unfortunately, any data about molecular aspects of kinetosome biogenesis in
473   invertebrates are absent. This fact and also the lack of the information about kinetosome
474   biogenesis in many groups of invertebrates, prevent us from any further comparisons and
475   speculations.

476   **Tentacles regeneration**

477   This study demonstrated that microsurgical amputation of distal part of tentacle(s) results
478   in the reparation of damaged tentacles and does not cause an extra cycle of degeneration-
479   regeneration of the whole polypide. It is interesting that only E-cells (abfrontal non-ciliated cells)
480   located at the wound edge are responsible for its healing. Labeling with EdU demonstrates that
481   the wound causes their dedifferentiation and limited proliferation from 1st to 5th day after surgery
482   (Fig. 12) to produce cells providing wound closure. In intact tentacles (in both experimental and
483   control polypides), epidermal cells never incorporate EdU. The ciliated cells of the tentacles are
484   very specialized and unable to proliferate even under the necessity of wound healing.
485   Surprisingly, regenerating tentacles in polypides of *E. pilosa* did not even considerably
486   lengthened by the 7th day after surgery. This contrasts with the data obtained from
487   plylactolaemates (Otto, 1921; Oda, 1954) whose tentacles restore their length in about 10 days.
488   We suggest that the tentacle recover its length according to a mechanism similar to normal
489   growth, powered by cell proliferation both in the ciliated pits and the oral region. We did not
490   statistically analyze proliferating activity at the lophophore base since our study is qualitative
491   and this is the first attempt to test the ability of tentacle regeneration in marine bryozoans.

492   Among the different variants of regeneration processes in animals, two main types are
493   recognized: epimorphosis and morphallaxis (Agata, Saito & Nakajima, 2007). During
494   epimorphosis, the cells of the residual part of the organ dedifferentiate and form a temporary
495   structure – the blastema. The dedifferentiated cells proliferate in the blastema and produce
496   material for *de novo* formation of the lost part of the organ. Alternatively, no blastema is formed
497   during morphollaxis, and regeneration of the lost body part is accomplished through remodeling
498   of the remaining part of the body. In this case, there is no accumulation of undifferentiated cells
499   or specific site of massive proliferation. According to our data, the regeneration of tentacles in *E.*
500   *pilosa* is similar to the morphollaxis type. Cellular mechanisms, de- and transdifferentiation
501   events remain to be described in the future studies.

502

Conclusions

504   This study demonstrates that the specific design of the bryozoan lophophore base enable
505 intercalary growth of tentacles. Using TEM and EdU-labeling, we detected the presence of stem
506 cells within the ciliated pits and the oral region of polypides and never within tentacles of adult
507 polypides. Cells of the ciliated pits are the source for the cells composing the lateral tentacle
508 surfaces, while the cells of the frontal tentacle surface originate from proliferating cells of the
509 oral region. Thus, the ciliated pits and the oral region of polypide are specific sites responsible
510 for the tentacle elongation. This confirmed the hypothesis that cell proliferation during tentacle
511 elongation takes place at the lophophore base and hence provides an opportunity of the tentacle
512 elongation in adult polypides without interfering with the feeding process. Such a potential to
513 alter the lophophore shape is crucial for encrusting colonies when they require the rearrangement
514 of colony-wide water currents with time. For the first time in prospective multiciliated epithelial
515 cells in invertebrates, we registered deuterosome-like structures during the kinetosome
516 biogenesis. Experiments on tentacle regeneration in *Electra pilosa* demonstrated that among all
517 types of epidermal cell, only abfrontal non-ciliated E-cells are responsible for wound healing.
518 Ciliated cells on the frontal and lateral tentacle surfaces are very specialized and unable to
519 proliferate even under the necessity of wound healing. The regeneration of tentacles is very slow
520 and similar to the morphollaxis type. We suggest that the tentacle recovers its length by a
521 mechanism similar to normal growth, powered by proliferation of cells both in the ciliated pits
522 and the oral region.

Acknowledgements

524   We sincerely thank Sergey Bagrov for help with sampling and Dr. Andrej Dobrovolskij
525 for inspiring discussion and valuable comments (both – Saint-Petersburg State University).
526 Gratitude is due to the Research and Educational Station "Belomorskaia" (former Marine
527 Biological Station) of Saint Petersburg University for hospitality. The study was partly done at
528 the Research center "Molecular and Cell Technologies" (Saint Petersburg State University).
529

References

531 Agata K, Saito Y, Nakajima E. Unifying principles of regeneration I: Epimorphosis versus
532   morphallaxis. Development, growth & differentiation. 2007;49(2):73-8.
533 Al Jord A, Lemaître AI, Delgehyr N, Faucourt M, Spassky N, Meunier A. Centriole
534   amplification by mother and daughter centrioles differs in multiciliated cells. Nature.
535   2014;516(7529):104.
536 Alexander BE, Liebrand K, Osinga R, Van Der Geest HG, Admiraal W, Cleutjens JP, Schutte B,
537   Verheyen F, Ribes M, Van Loon E, De Goeij JM. 2014. Cell turnover and detritus
538   production in marine sponges from tropical and temperate benthic ecosystems. PLOS ONE
539   9(10):e109486
540 Anderson RG, Brenner RM. The formation of basal bodies (centrioles) in the Rhesus monkey
541   oviduct. The Journal of cell biology. 1971;50(1):10–34.
542 Ash BM, Stephens RE. Ciliogenesis during the sequential formation of molluscan gill filaments.
543   Developmental biology. 1975;43(2):340–7.

544 Balestra FR, Gönczy P. Multiciliogenesis: multicilin directs transcriptional activation of centriole
545   formation. Current Biology. 2014;24(16):R746–9.
546 Banta WC, McKinney FK, Zimmer RL. Bryozoan monticules: excurrent water outlets? Science.
547   1974;185(4153):783–4.
548 Baonza A, Freeman M. Control of cell proliferation in the Drosophila eye by Notch signaling.
549   Developmental cell. 2005;8(4):529-39.
550 Bely AE. Early events in annelid regeneration: a cellular perspective. *Integrative and*
551   *Comparative Biology*, 2014;54(4):688–699.
552 Berning B. Evidence for sublethal predation and regeneration among living and fossil
553   ascophoran bryozoans. Bryozoan studies. 2007:1-7.
554 Bettencourt-Dias M, Mittnacht S, Brockes JP. Heterogeneous proliferative potential in
555   regenerative adult newt cardiomyocytes. Journal of cell science. 2003;116(19):4001-9.
556 Brinkmann N, Wanninger A. Integrative analysis of polychaete ontogeny: cell proliferation
557   patterns and myogenesis in trochophore larvae of Sabellaria alveolata. Evolution &
558   development. 2010;12(1):5-15.
559 Borisenko IE, Adamska M, Tokina DB, Ereskovsky AV. Transdifferentiation is a driving force
560   of regeneration in Halisarca dujardini (Demospongiae, Porifera). PeerJ. 2015;3:e1211.
561   https://doi.org/10.7717/PeerJ.1211.
562 Cebrià F, Adell T, Saló E. Rebuilding a planarian: from early signaling to final shape.
563   International Journal of Developmental Biology. 2018;62(6-7-8):537-50.
564 Chera S, Ghila L, Dobretz K, Wenger Y, Bauer C, Buzgariu W, Martinou J-C, Galliot B.
565   Apoptotic cells provide an unexpected source of Wnt3 signaling to drive hydra head
566   regeneration. Developmental Cell. 2009;17(2):279–289
567 Cifrian B, García-Corrales P, Martínez-Alos S. Intracytoplasmic ciliary elements in epidermal
568   cells of Syndesmis echinorum and Paravortex cardii (Platyhelminthes, Dalyellioida).
569   Journal of morphology. 1992;213(2):147–57.
570 Cook PL. Colony-wide water currents in living Bryozoa. Cahiers de Biologie Marine.
571   1977;18:31-47.
572 Cook PL, Chimonides PJ. Further observations on water current patterns in living Bryozoa.
573   Cahiers de Biologie Marine. 1980;21:393–402.
574 Dick MH. A proposed mechanism for chimney formation in encrusting bryozoan colonies. In:
575   Ross JRP, editor. Bryozoa: present and past. Bellingham: Western Washington University;
576   1987. p 73–80.
577 Dirksen ER. Centriole morphogenesis in developing ciliated epithelium of the mouse oviduct.
578   The Journal of cell biology. 1971;51(1):286–302.
579 Dirksen ER. Centriole and basal body formation during ciliogenesis revisited. Biology of the
580   Cell. 1991;72(1-2):31–8.
581 Drobysheva IM. Centriole formation in insunk epidermis of Geocentrophora wagini
582   (Lecithoepitheliata, Plathelminthes). Doklady Biological Sciences. 2006;409(1):351–353.
583 Drobysheva IM. Replication of basal bodies during ciliogenesis in the epidermis of
584   Prolecithophora and Lecithoepitheliata (Plathelminthes). Belg. J. Zool. 2010;140
585   (Suppl.):127–131.
586 Ereskovsky AV, Borisenko IE, Lapébie P, Gazave E, Tokina DB, Borchiellini C. Oscarella
587   lobularis (Homoscleromorpha, Porifera) Regeneration: Epithelial Morphogenesis and
588   Metaplasia. PLoS ONE. 2015;10(8), e0134566.

589   Fischer A, Dorresteijn A. The polychaete Platynereis dumerilii (Annelida): a laboratory animal
590   with spiralian cleavage, lifelong segment proliferation and a mixed benthic/pelagic life
591   cycle. BioEssays. 2004;26(3):314-25.
592   Fritz AE, Ikmi A, Seidel C, Paulson A, Gibson MC. Mechanisms of tentacle morphogenesis in
593   the sea anemone Nematostella vectensis. Development . 2013;140(10):2212–2223
594   Gahan JM, Bradshaw B, Flici H, Frank U. The interstitial stem cells in Hydractinia and their role
595   in regeneration. Current Opinion in Genetics & Development. 2016; 40:65–73
596   Gordon DP. Microarchitecture and function of the lophophore in the bryozoan Cryptosula
597   pallasiana. Marine Biology. 1974;27(2):147–163.
598   Grdisa M. Mechanism of wound healing in annelids. Invertebrate Survival Journal.
599   2010;7(2):192-7.
600   Grimaldi A, Tettamanti G, Rinaldi L, Brivio MF, Castellani D, De Eguileor M. Muscle
601   differentiation in tentacles of Sepia officinalis (Mollusca) is regulated by muscle regulatory
602   factors (MRF) related proteins. Development, growth & differentiation. 2004;46(1):83-95.
603   Hagiwara H, Ohwada N, Takata K. Cell biology of normal and abnormal ciliogenesis in the
604   ciliated epithelium. International review of cytology. 2004;234:101–41.
605   Hagiwara H, Ohwada N, Aoki T, Takata K. Ciliogenesis and ciliary abnormalities. Medical
606   Electron Microscopy. 2000;33(3):109–14.
607   Hay ED, Fischman DA. Origin of the blastema in regenerating limbs of the newt Triturus
608   viridescens: An autoradiographic study using tritiated thymidine to follow cell proliferation
609   and migration. Developmental biology. 1961 Feb 1;3(1):26-59.
610   Henry JQ, Okusu A, Martindale MQ. The cell lineage of the polyplacophoran, Chaetopleura
611   apiculata: variation in the spiralian program and implications for molluscan evolution.
612   Developmental biology. 2004;272(1):145-60.
613   Iyengar EV, Harvell CD. Specificity of cues inducing defensive spines in the bryozoan
614   Membranipora membranacea. Marine Ecology Progress Series. 2002;225:205-18.
615   Jørgensen CB. Biology of suspension feeding. Oxford-London-New York-Paris: Pergamon
616   Press; 1966.
617   Kahn AS, Leys SP. The role of cell replacement in benthic–pelagic coupling by suspension
618   feeders. Royal Society Open Science. 2016;3(11):160484
619   Kalnins V. Ultrastructural observations on development of cilia in trochophore of Nereis limbata.
620   Biological Bulletin. 1967;133(2):472.
621   Lidgard S. Water flow, feeding, and colony form in an encrusting cheilostome. In: Larwood GP,
622   Nielsen C, editors. Recent and Fossil Bryozoa. Fredensborg, Denmark: Olsen and Olsen;
623   1981. p. 135–142.
624   Lidgard S. Predation on marine bryozoan colonies: taxa, traits and trophic groups. Marine
625   Ecology Progress Series. 2008;359:117-31.
626   Lindsay SM. Frequency of injury and the ecology of regeneration in marine benthic
627   invertebrates. Integrative and Comparative Biology. 2010;50(4):479-93.
628   Lutaud G. L'innervation du lophophore chez le bryozoaire chilostome Electra pilosa (L.).
629   Zeitschrift fur Zellforschung und mikroskopische Anatomie. 1973 ;140 :217–234.
630   Marcus E. Sôbre bryozoa do Brasil. Bolm Fac fil ciénc letr Univ Sao Paolo, Zool. 1941;5:3–208.
631   Matricon I. Dégénérescence du polypide femelle et formation d'une poche incubatrice chez
632   Alcyonidium polyoum (Hassall)(Bryozoaire Cténostome). Arc Zool Exp Gén.
633   1963;102:79–93.

634 McKinney FK. Feeding and associated colonial morphology in marine bryozoans. Critical
635   Reviews in Aquatic Sciences. 1990;2(2):255-280.
636 Milán M, Campuzano S, García-Bellido A. Cell cycling and patterned cell proliferation in the
637   Drosophila wing during metamorphosis. Proceedings of the National Academy of Sciences.
638   1996;93(21):11687-92.
639 Mukai H, Terakado K, Reed CG. Bryozoa. In Harrison FW, Woollacott RM, editors.
640   Microscopic anatomy of invertebrates, vol 13. New York: Wiley-Liss; 1997. p.45–206.
641 Nabais C, Pereira SG, Bettencourt-Dias M. Noncanonical biogenesis of centrioles and basal
642   bodies. In: Cold Spring Harbor symposia on quantitative biology. New-York: Cold Spring
643   Harbor Laboratory Press. 2017; Vol. 82:123–135.
644 Neufeld TP, De La Cruz AF, Johnston LA, Edgar BA. Coordination of growth and cell division
645   in the Drosophila wing. Cell. 1998;93(7):1183-93.
646 Oda S. Radiosensitivity in Lophopodella carteri, a freshwater Bryozoan. Science Reports of the
647   Tokyo Bunrika Daigaku, B. 1954;7:211–217.
648 Otto F. Studien über das Regulationsvermögen einiger Süßwasserbryozoen. Development Genes
649   and Evolution. 1921;47(3):399–442.
650 Pardos F, Roldan C, Benito J, Emig CC. Fine structure of the tentacles of Phoronis australis
651   Haswell (Phoronida, Lophophorata). Acta Zoologica. 1991;72(2):81–90.
652 Paulus T, Müller MC. Cell proliferation dynamics and morphological differentiation during
653   regeneration in Dorvillea bermudensis (Polychaeta, Dorvilleidae). Journal of morphology.
654   2006;267(4):393-403.
655 Reddien PW, Alvarado AS. Fundamentals of planarian regeneration. Annu. Rev. Cell Dev. Biol..
656   2004; 20:725-57.
657 Redl E, Scherholz M, Wollesen T, Todt C, Wanninger A. Cell proliferation pattern and twist
658   expression in an aplacophoran mollusk argue against segmented ancestry of Mollusca.
659   Journal of Experimental Zoology Part B: Molecular and Developmental Evolution.
660   2016;326(7):422-36.
661 Salic A, Mitchison TJ. A chemical method for fast and sensitive detection of DNA synthesis in
662   vivo. Proceedings of the National Academy of Sciences. 2008;105(7):2415-20.
663 Saló E, Abril JF, Adell T, Cebriá F, Eckelt K, Fernández-Taboada E, Handberg-Thorsager M,
664   Iglesias M, Molina MD, Rodríguez-Esteban G. Planarian regeneration: achievements and
665   future directions after 20 years of research. International Journal of Developmental
666   Biology. 2009;53(8-9-10):1317-27.
667 Schwaha T, Bernhard JM, Edgcomb VP, Todaro MA. Aethozooides uraniae, a new deep-sea
668   genus and species of solitary bryozoan from the Mediterranean Sea, with a revision of the
669   Aethozoidae. Marine Biodiversity. 2019 Aug 1;49(4):1843-56.
670 Schwaha T, Wood TS. Organogenesis during budding and lophophoral morphology of Hislopia
671   malayensis Annandale, 1916 (Bryozoa, Ctenostomata). BMC developmental biology.
672   2011;11(1):23.
673 Shahid U, Singh P. Emerging Picture of Deuterosome-Dependent Centriole Amplification in
674   MCCs. Cells. 2018;7(10):152.
675 Shunatova NN, Nielsen C. Putative sensory structures in marine bryozoans. Invertebrate
676   Biology. 2002;121(3):262–70.
677 Shunatova N, Tamberg Y. Body cavities in bryozoans: Functional and phylogenetic implications.
678   Journal of morphology. 2019;280(9):1332–58.

679 Smith LW. (1973). Ultrastructure of the tentacles of Flustrellidra hispida (Fabricius). In G. P.
680   Larwood, editor. Living and fossil bryozoa. New York: Academic Press; 1973. p. 335–
681   342.
682 Sorokin SP. Reconstructions of centriole formation and ciliogenesis in mammalian lungs.
683   Journal of cell science. 1968;3(2):207–30.
684 Spassky N, Meunier A. The development and functions of multiciliated epithelia. Nature reviews
685   Molecular cell biology. 2017;18(7):423.
686 Tamm SI, Tamm SL. Development of macrociliary cells in Beroe. I. Actin bundles and centriole
687   migration. Journal of cell science. 1988;89(1):67–80.
688 Tyler S. Development of cilia in embryos of the turbellarian Macrostomum. In: The Biology of
689   the Turbellaria. Dordrecht: Springer; 1981. p. 231–239.
690 Tyler S. Ciliogenesis in embryos of the acoel turbellarian Archaphanostoma. Transactions of the
691   American Microscopical Society. 1984;1:1–5.
692 von Dassow M. Effects of ambient flow and injury on the morphology of a fluid transport system
693   in a bryozoan. The Biological Bulletin. 2005a;208(1):47–59.
694 von Dassow M. Flow and conduit formation in the external fluid-transport system of a
695   suspension feeder. Journal of Experimental Biology. 2005b;208(15):2931–2938.
696 von Dassow M. Function-dependent development in a colonial animal. The Biological Bulletin.
697   2006;211(1):76–82.
698 Waeschenbach A, Taylor PD, Littlewood DT. A molecular phylogeny of bryozoans. Molecular
699   Phylogenetics and Evolution. 2012; 62(2):718–35.
700 Warren M, Puskarczyk K, Chapman SC. Chick embryo proliferation studies using EdU labeling.
701   Developmental Dynamics. 2009;238(4):944-9.
702 Winston JE. Polypide morphology and feeding behavior in marine ectoprocts. Bulletin of Marine
703   Science. 1978;28(1):1–31.
704 Winston JE. Current-related morphology and behaviour in some Pacific coast bryozoans.
705   Advances in bryozoology. 1979;13:247–68.
706 Yan X, Zhao H, Zhu X. Production of basal bodies in bulk for dense multicilia formation.
707   F1000Research. 2016;5.
708 Yoshida-Noro C, Tochinai S. Stem cell system in asexual and sexual reproduction of
709   Enchytraeus japonensis (Oligochaeta, Annelida). Development, growth & differentiation.
710   2010;52(1):43-55.
711 Zhao H, Zhu L, Zhu Y, Cao J, Li S, Huang Q, Xu T, Huang X, Yan X, Zhu X. The Cep63
712   paralogue Deup1 enables massive de novo centriole biogenesis for vertebrate
713   multiciliogenesis. Nature cell biology. 2013;15(12):1434.

Figure 1

Figure 1: General structure of tentacles in gymnolaemates.

(A) Feeding colony of *Electra pilosa* (in life). Note the funnel shape of lophophores. (B) Cross-section of the tentacle in *Eucratea loricata* (TEM; the frontal surface of the tentacle to the bottom left). (C) A schematic drawing of tentacle cross-section demonstrating an alphabetical code referring to different cell types (the frontal surface of the tentacle to the bottom). (D) Tentacle ciliation in *Aquiloniella scabra* (SEM; lateral view of the tentacle) showing lateral, latero-frontal and frontal ciliary bands. Abbreviations: A – frontal cell (A-cell), B – latero-frontal cell (B-cell), C – fronto-lateral cell (C-cell), D – abfronto-lateral cell (D-cell), E – abfrontal cell (E-cell), F – putative sensory cell (F-cell) forming intermittent row at the midline of the abfrontal tentacle surface, anb – abfrontal nerve bundle, cu – cuticle, ECM – extracellular matrix, fc – frontal ciliary band, fnb – frontal nerve bundle, lc – lateral ciliary band, lfc – latero-frontal ciliary band, lfnb – latero-frontal nerve bundle, tc – lumen of the tentacle coelom.
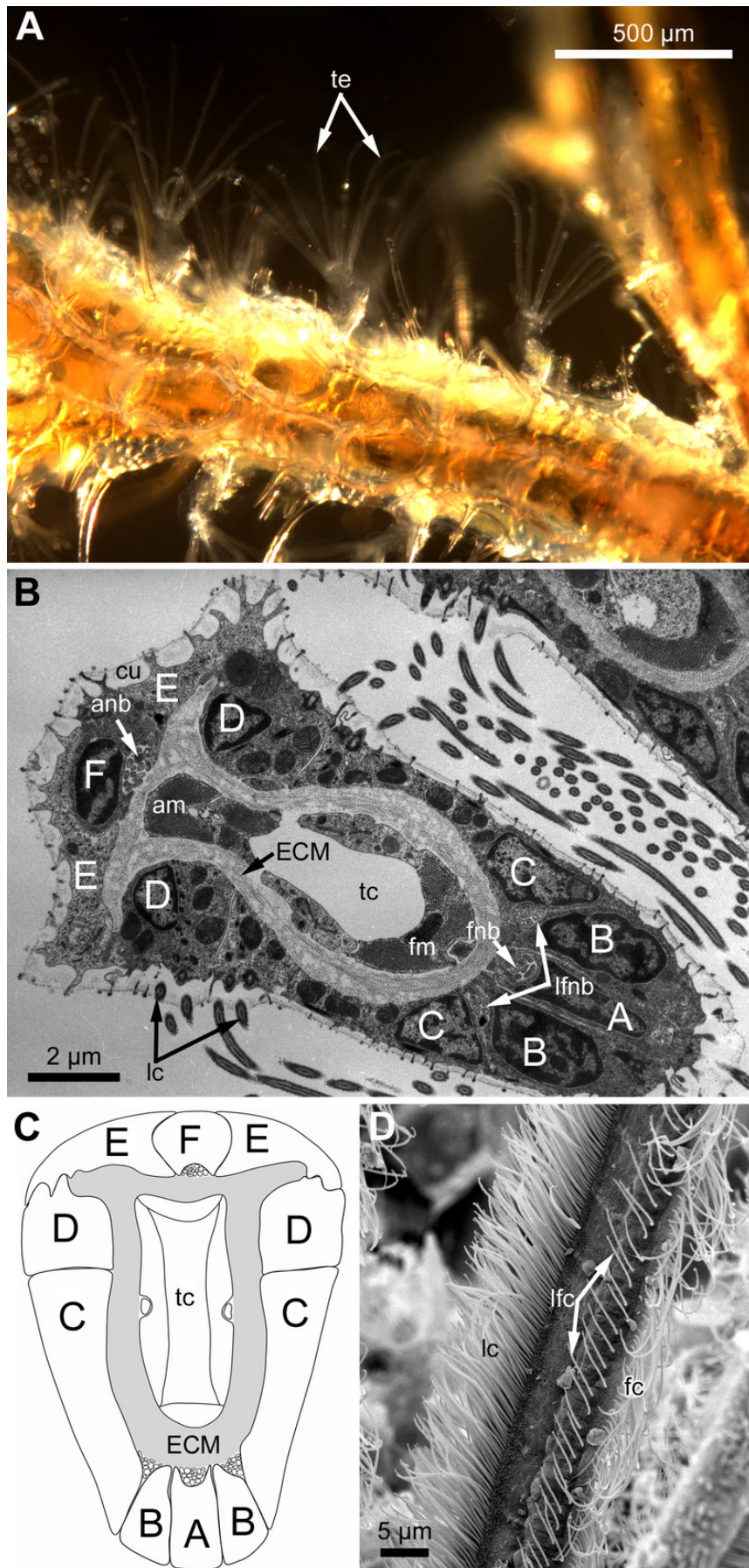
Figure 2

Figure 2: Arrangement of mono- and multiciliated F-cells in young (2nd age class) and adult (5th age class) polypides of *Aquiloniella scabra*.

(A) The distal part of the tentacle in adult polypide (SEM; abfrontal view). Note the regular arrangement of mono- (*arrowhead*) and multiciliated (*double arrowhead*) F-cells. (B) The basal part of the tentacle in adult polypide (SEM; abfrontal view). Note a single multiciliated F-cell at the tentacle base. (C) The basal part of the tentacle in young polypide (SEM; abfrontal view). Note the tightly packed mono- (*arrowheads*) and multiciliated (*double arrowheads*) F-cells at the tentacle base.
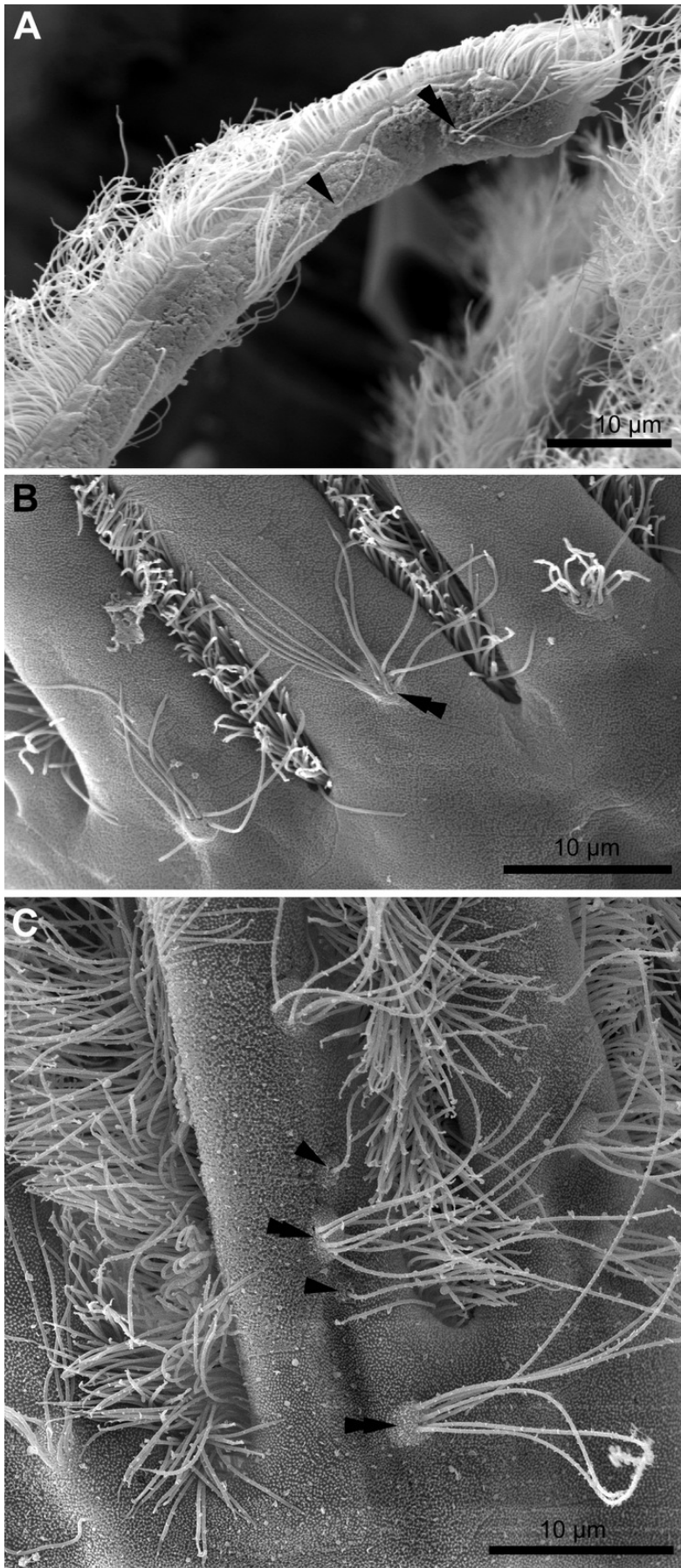
Figure 3

Figure 3: Microanatomy of the lophophore base at the level of the ciliated pits' openings.

(A–D) Oblique-cross sections of the lophophore base of adult polypide in *Aquiloniella scabra* (TEM); (E–F) longitudinal semi-thin section of adult polypide in *Rhamphostomella ovata*. (A) At the proximal end of the tentacle, the number of E-cells increases from two to three, and they combine both with the epidermis of the tentacle sheath and with the E-cells of the adjoining tentacles. The white frame corresponds to the enlarged area in (B); the black frame corresponds to the enlarged area in (C). (B) The enlarged area in (A), demonstrating thin projections of the tentacle ECM (*arrowheads*) enveloping the basal portions of E-cells. (C) Enlargement of (A), demonstrating thin projections of the tentacle ECM uniting with the ECM of the septum dividing the lophophore and main body cavity. (D) B- and C-cells of adjacent tentacles contact each other and isolate the lumen of the ciliated pit. (E) Longitudinal semi-thin section through the ciliated pit which is a blind-ended conical invagination of the epidermis. The black frame corresponds to the enlarged area in (F). (F) The enlarged area in (E), demonstrating three regions along the axis of the ciliated pit. Note the mitotic figure in the proximal part of the ciliated pit. Abbreviations: A – frontal cell (A-cell), B – latero-frontal cell (B-cell), C – fronto-lateral cell (C-cell), D – abfronto-lateral cell (D-cell), E – abfrontal cell (E-cell), alh – abfronto-lateral horns of tentacle ECM, anb – abfrontal nerve bundle, cp – ciliated pit, cpo – opening of the ciliated pit, cu – cuticle, dp – distal part of the ciliated pit, ECM – extracellular matrix, ga – ganglion, mi – mitotic figure, mo – mouth, mp – middle part of the ciliated pit, pp – proximal part of the ciliated pit, pr – additional projections of the tentacle ECM, se – septum dividing the lophophore and main body cavity, tc – tentacle coelom, trc – main body cavity, tsh – tentacle sheath.
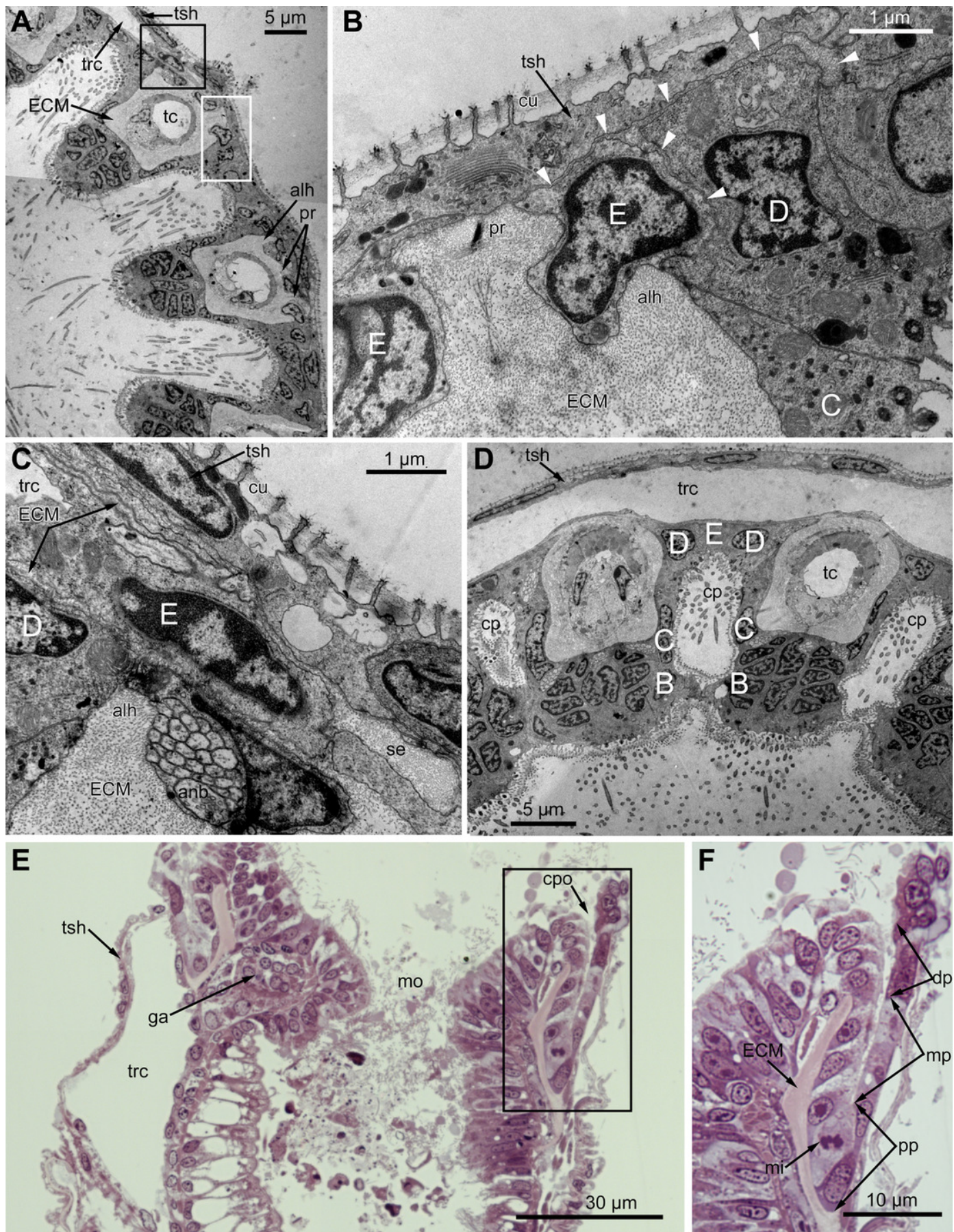
Figure 4

Figure 4: A schematic drawing of the ciliated pit in *Rhamphostomella ovata*.

A sector of the lophophore base is shown (mouth area to the left). Tentacles are cut at the bases at the level of the opening of ciliated pits. Cilia are not shown. The cells of the ciliated pit are colored in light green; epidermal cells of the tentacle sheath and the oral region are shaded in light blue; extracellular matrix is light grey; cells of coelomic lining are light yellow. Color code for nuclei: orange for CP-cells, green for DP-cells, violet for EP cells, dark grey for P-cells, grey for the rest of the cells.

Abbreviations: CP and DP – vertical rows of the cells composing the lateral walls of the ciliated pit and located below the corresponding C- and D-cells of the neighboring tentacles; EP – cells composing the abfrontal surface of the ciliated pit; PC – P-cells (cells located in the proximal region of the ciliated pit); cpo – ciliated pit opening, dls – deuterosome-like structures, ECM – extracellular matrix, epi – epiperitoneal cell lining lateral surface of the tentacle coelom, ik – irregularly arranged kinetosomes, mi – mitotic figures, sub – subperitoneal cell of the tentacle coelomic lining, tc – tentacle coelom, trc – main body cavity, tsh – tentacle sheath.
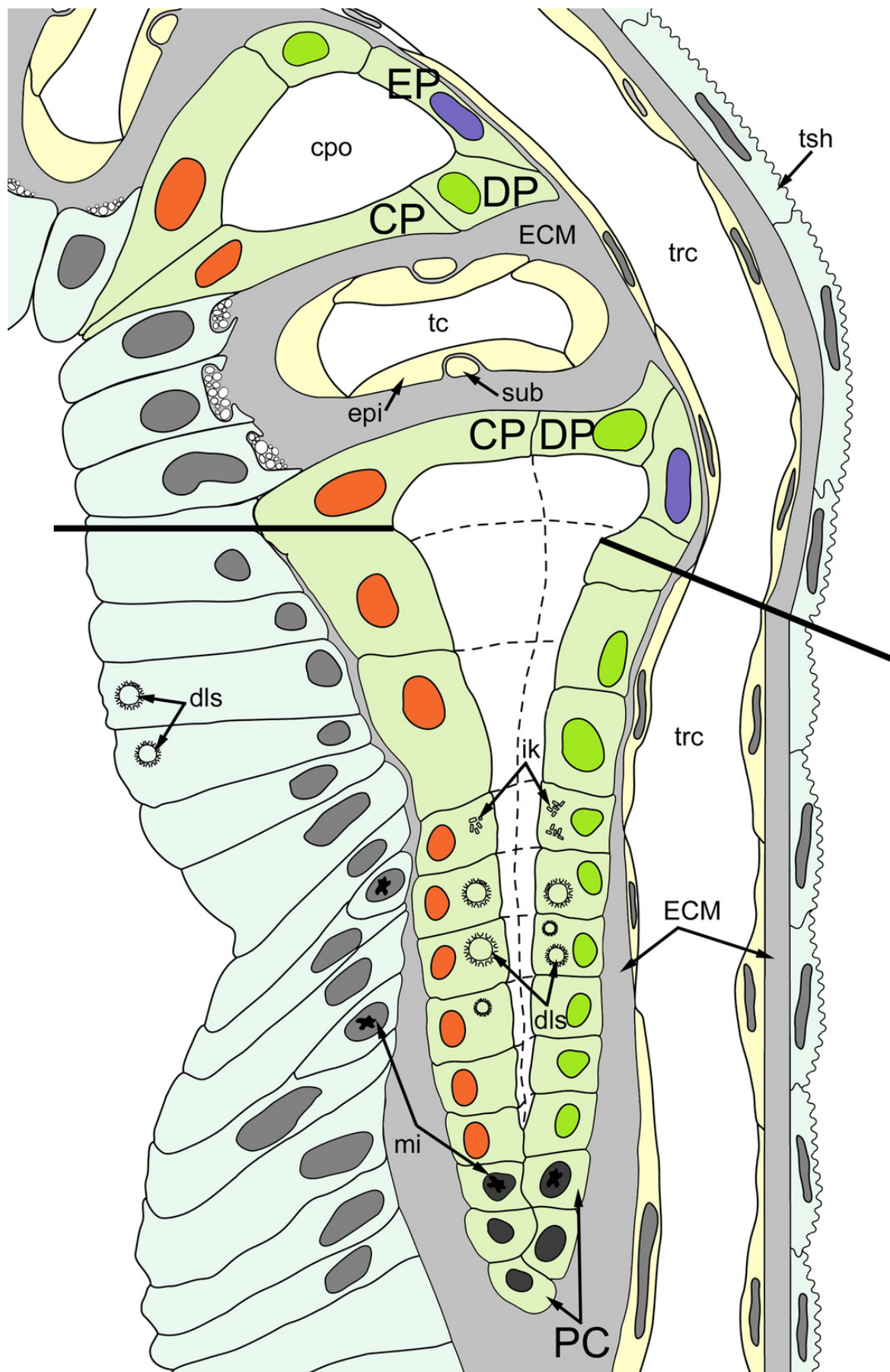
Figure 5

Figure 5: Fine structure of the distal region of the ciliated pits (TEM; oblique-cross sections of the lophophore base).

(A) Details of the basal complex in CP- and DP-cells located close to the opening of the ciliated pit (*Aquiloniella scabra*; mouth upwards). (B) The fine structure of CP-cells located close to the ciliated pit opening (*Rhamphostomella ovata*; mouth upwards). (C) CP- and DP-cells located at the border with the middle region of the ciliated pit possess fewer cilia (*A.scabra*; mouth upwards). (D) The ultrastructure of EP-cells (*A.scabra*; mouth upwards). Abbreviations: CP and DP – vertical rows of the cells composing the lateral walls of the ciliated pit and located below the corresponding C- and D-cells of the neighboring tentacles; EP – cells composing the abfrontal surface of the ciliated pit; ar – axial rootlet, ci – cilium, cu – cuticle, dG – dictyosome of Goldgi complex, ECM – extracellular matrix, k – kinetosome, lr – lateral rootlet, lu – lumen of the ciliated pit, m – mitochondrion, nb – nerve bundle, trc – main body cavity.
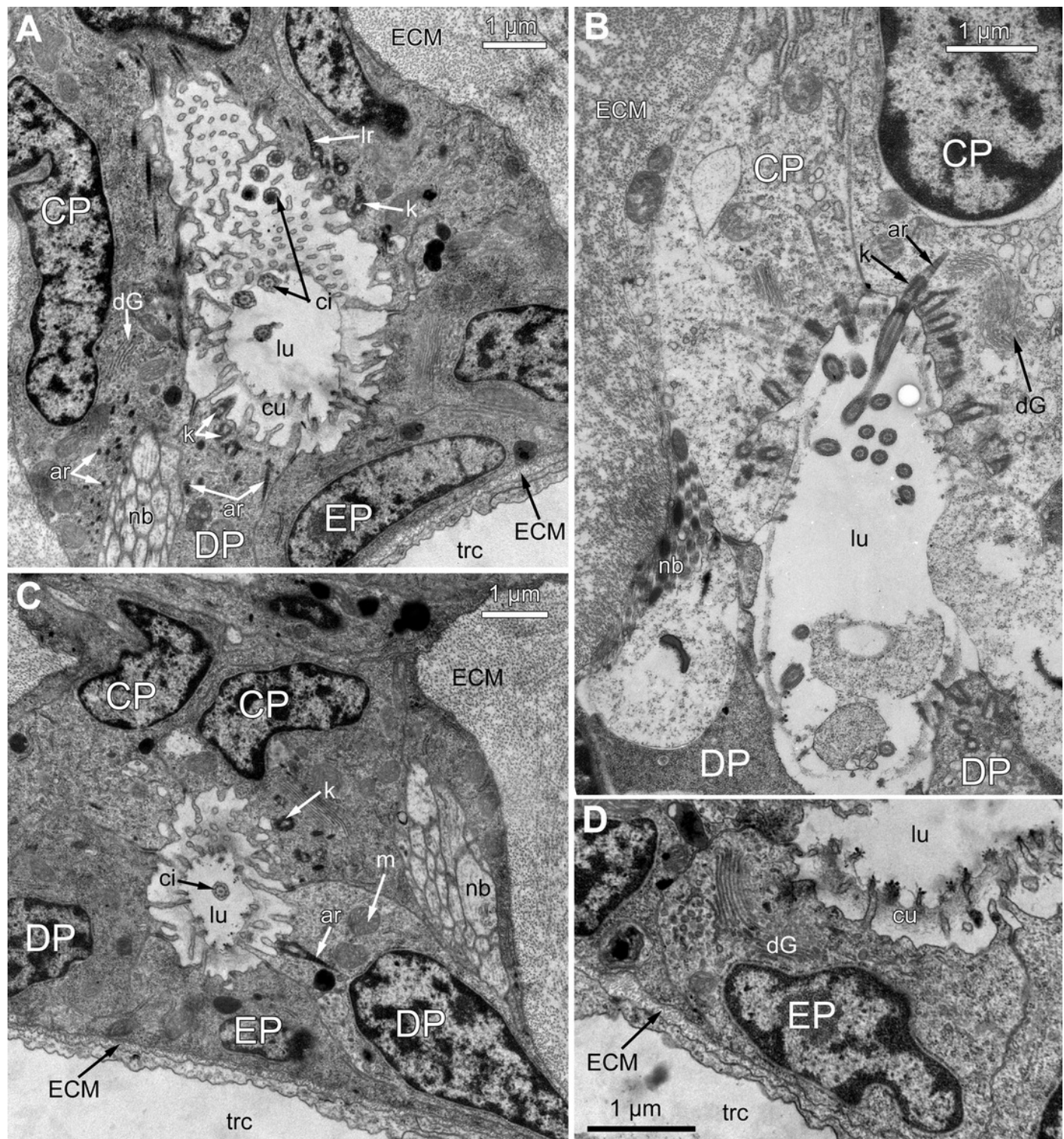
Figure 6

Figure 6: The fine structure of the middle region of the ciliated pits (TEM; oblique cross-sections of the lophophore base in polypide of 3rd age class).

(A) There is a single cilium within the lumen of the ciliated pit (*Aquiloniella scabra*; mouth left upwards). Note the deuterosome-like structure in the DP-cell. (B) The apical part of CP-cell contains numerous irregularly arranged kinetosomes (*Eucratea loricata*; mouth to the right). (C–F): different stages if kinetosome biogenesis in young polypide of *Rhamhostomella ovata*. (C) Clusters of electron-dense 'fibrogranular material' and deuterosome-like structures in the apical parts of both CP- and DP-cells (mouth upwards). (D) The apical part of DP-cell contains vacuoles with fibrillar electron-dense or electron-lucent content (mouth upwards). (E) Deuterosome-like structures and developing cross-striated rootlets surrounded by electron-dense 'fibrogranular material' (mouth to the right). Note that one of the procentrioles (*double arrowhead*) is larger and lies at the right angle to the rest. (F) Late stages of kinetosome biogenesis in DP-cells: one cell contains free procentrioles and 'fibrogranular material', the other has irregularly arranged kinetosomes, some of them with axial rootlet (mouth to the right). Abbreviations: CP and DP – vertical rows of the cells composing the lateral walls of the ciliated pit and located below the corresponding C- and D-cells of the neighboring tentacles; EP – cells composing the abfrontal surface of the ciliated pit; ar – axial rootlet, ci – cilium, cu – cuticle, dG – dictyosome of Goldgi complex, dls – deuterosome-like structure, dr – developing rootlet, ECM – extracellular matrix, fg – 'fibrogranular material', k – kinetosome, lu – lumen of the ciliated pit, m – mitochondrion, nb – nerve bundle, pc – procentrioles, rER- rough endoplasmic reticulum, trc – main body cavity, vf – vacuoles with fibrillar electron-dense content, vl – vacuoles with electron-lucent content.
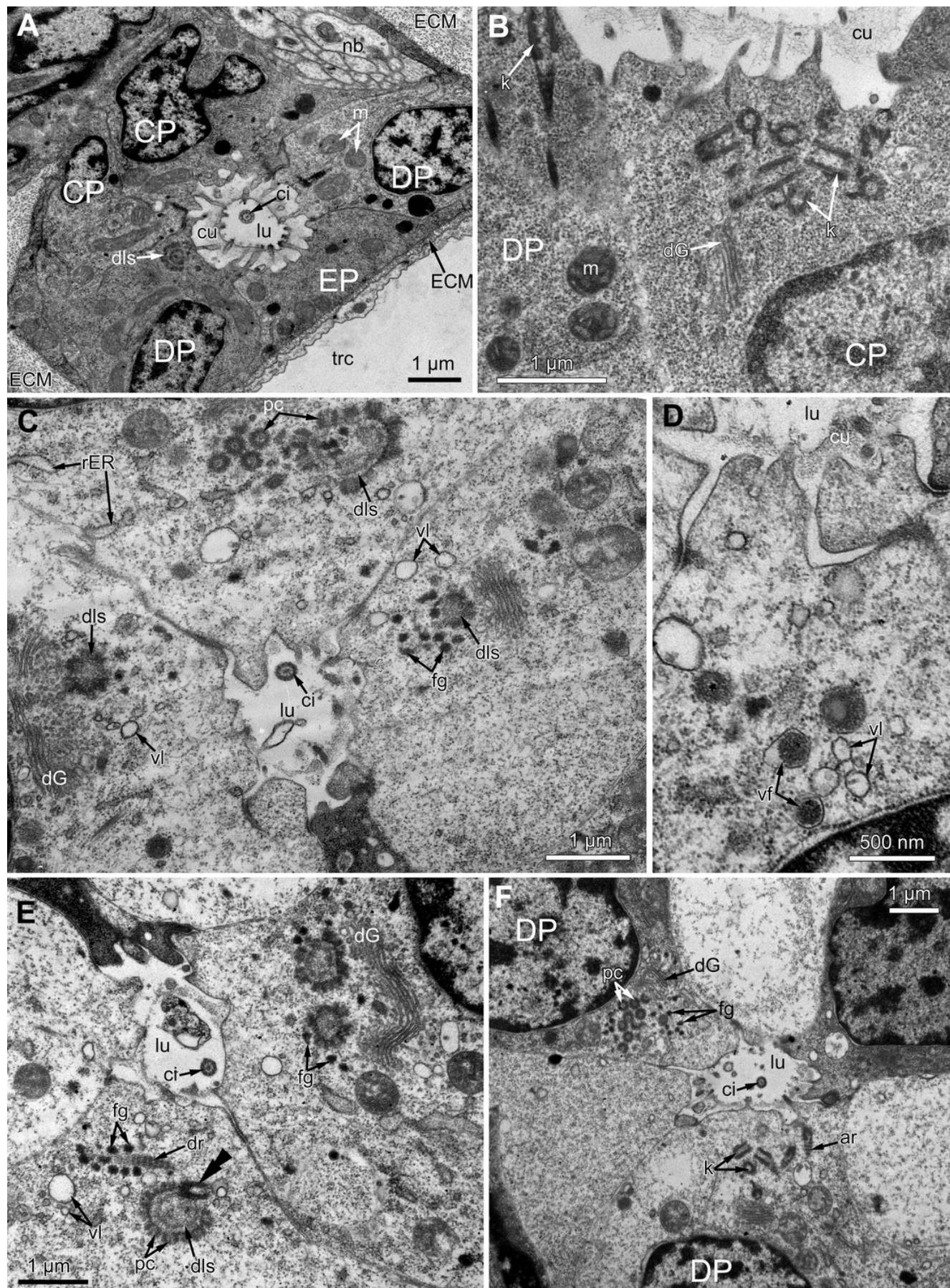
Figure 7

Figure 7: Microanatomy of the proximal region of the ciliated pits in the poypides of the 3rd age class: (A–B): *Aquiloniella scabra*; (C–E): *Rhamhostomella ovata.*

(A) Oblique-cross sections of the lophopore base (TEM; mouth downwards), showing three ciliated pits cut at different levels: close to the border with middle region (*arrowhead*), close to the bottom (*double arrowhead*), through the most basal P-cell (PL). (B) Ultrastructure of P-cells located close to the border with the middle region (oblique-cross sections of the lophopore base; TEM; mouth downwards). (C) Ultrastructure of P-cells at the bottom of the ciliated pit (oblique cross-sections of the lophopore base; TEM; mouth downwards). (D) Longitudinal semi-thin section of the polypide through the wall of the ciliated pit (tentacle tips upwards). The white frame corresponds to the enlarged area in (E). (E) Enlargement of (D), demonstrating mitotic figure within one of P-cells. Abbreviations: dG – dictyosome of Golgi complex, ECM – extracellular matrix, ER – endoplasmic reticulum, k – kinetosome, mi – mitotic figure, mo – mouth, phcm – circular muscles of the pharynx (pharynx constrictors), phw – epithelium of the pharynx, PL – the lowest P-cell at the bottom of ciliated pit, rc – ring coelomic canal of the lophophore, rcl – coelomic lining of the ring canal, te – tentacle, trc – main body cavity, tsh – tentacle sheath.
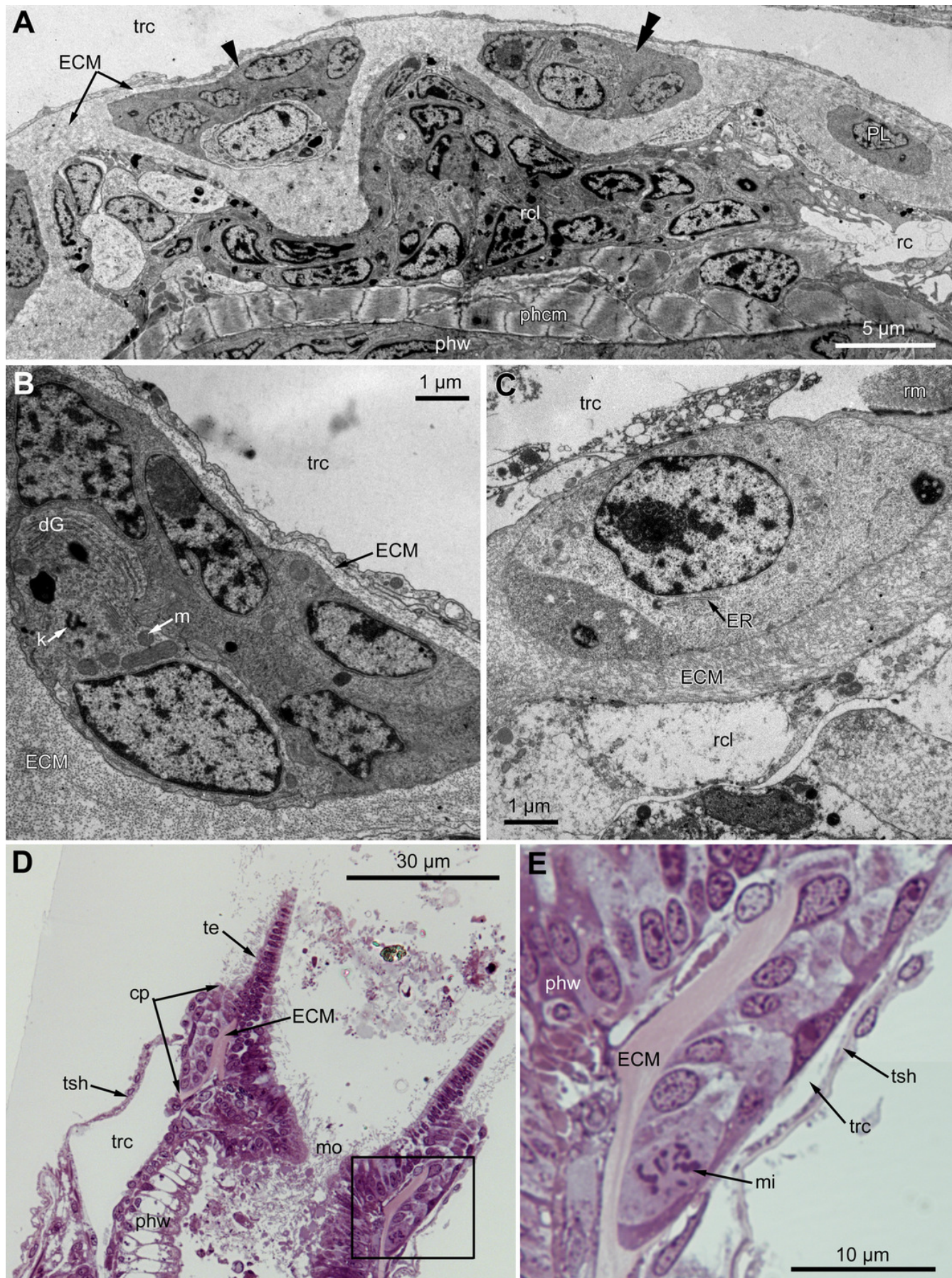
Figure 8

Figure 8: Microanatomy of the oral region: (A–C, E): *Aquiloniella scabra*; (C–D): *Eucratea loricata.*

(A) The frontal row of A-cells is two cells wide at the very base of the tentacles (cross section; TEM). (B) The tentacle bases and the oral region of the polypide (SEM). (C) Longitudinal section (TEM) of the polypide through the tentacle (left) and the ciliated pit (right). The white frame approximately corresponds to the outer rim shown in (D). The black frame approximately corresponds to the ciliated area of the oral region shown in (E). (D) The outer rim of the oral region lacks cilia and possesses long microvilli in *E.loricata* (SEM). (E) The fine structure of the ciliated cells of the oral region (oblique-cross section; TEM). Abbreviations: A – frontal cell (A-cell), B – latero-frontal cell (B-cell), C – fronto-lateral cell (C-cell), ar – axial rootlet, dG – dictyosome of Golgi complex, fc – frontal ciliary band, k – kinetosome, mo – mouth, mv – microvilli, or – oral region, phcm – circular muscles of the pharynx (pharynx constrictors), phw – epithelium of the pharynx, rc – ring coelomic canal of the lophophore, rim – outer rim of the oral region, se – septum dividing the lophophore and main body cavity, tc – tentacle coelom, trc – main body cavity, va – vacuole.
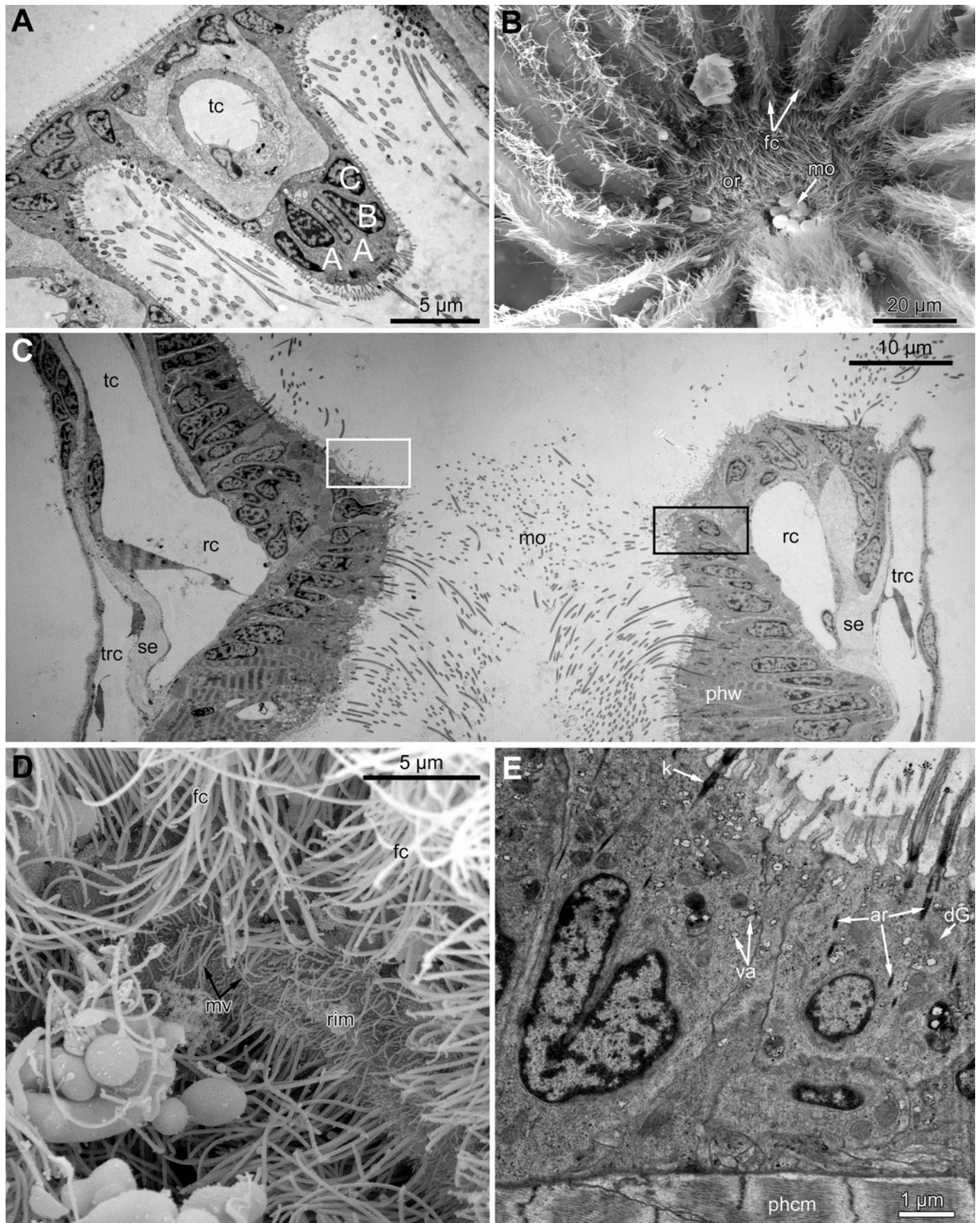
Figure 9

Figure 9: The fine structure of the oral region in the polypides of the 3rd and 4th age classes in *Rhamphostomella ovata.*

(A–B, E–F): cross sections of the lophophore base (TEM); (C–D): the oral region of polypide (SEM). (A) The oral region is composed of two cell types: ciliated cells with electron-dense cytoplasm (located in the continuation of the rows of A-cells) and non-ciliated cells with election-gray cytoplasm, forming small lobe-shaped apical projections. The tentacle coeloms are shaded in violet, the cells composing ciliated pits are shaded in cyan. The white frame corresponds to the enlarged area in (B). (B) Enlargement of (A), showing the fine structure of the ciliated cells of the oral region. Note cluster of 'fibrogranular materiall' in one of the non-ciliated cells. (C) General view of the oral region of polypide. Note the drop-shaped structures clogging the mouth. The black frame corresponds to enlarged area in (D). Inset: Drop-shaped structures have thin and short stalk. (D) Enlargement of (C), showing apical projections of putative secretory cells. (E) Details of kinetosome biogenesis in non-ciliated cells. Note that one of the procentrioles (*arrowhead*) is larger and lies at the right angle to the rest. (F) Cell undergoing mitosis (shaded in yellow). Abbreviations: ap – apical projection of putative secretory cell, ar – axial rootlet, cc – ciliated cells of the oral region, cu – cuticle, dG – dictyosome of Golgi complex, dls – deuterosome-like structures, dr – drop-shaped structures clogging the mouth, fc – frontal ciliary band, fg – 'fibrogranular material', k – kinetosome, lr – lateral rootlet, mo – mouth, or – oral region, pc – procentrioles, sc – putative secretory cell, trc – main body cavity, tsh – tentacle sheath.
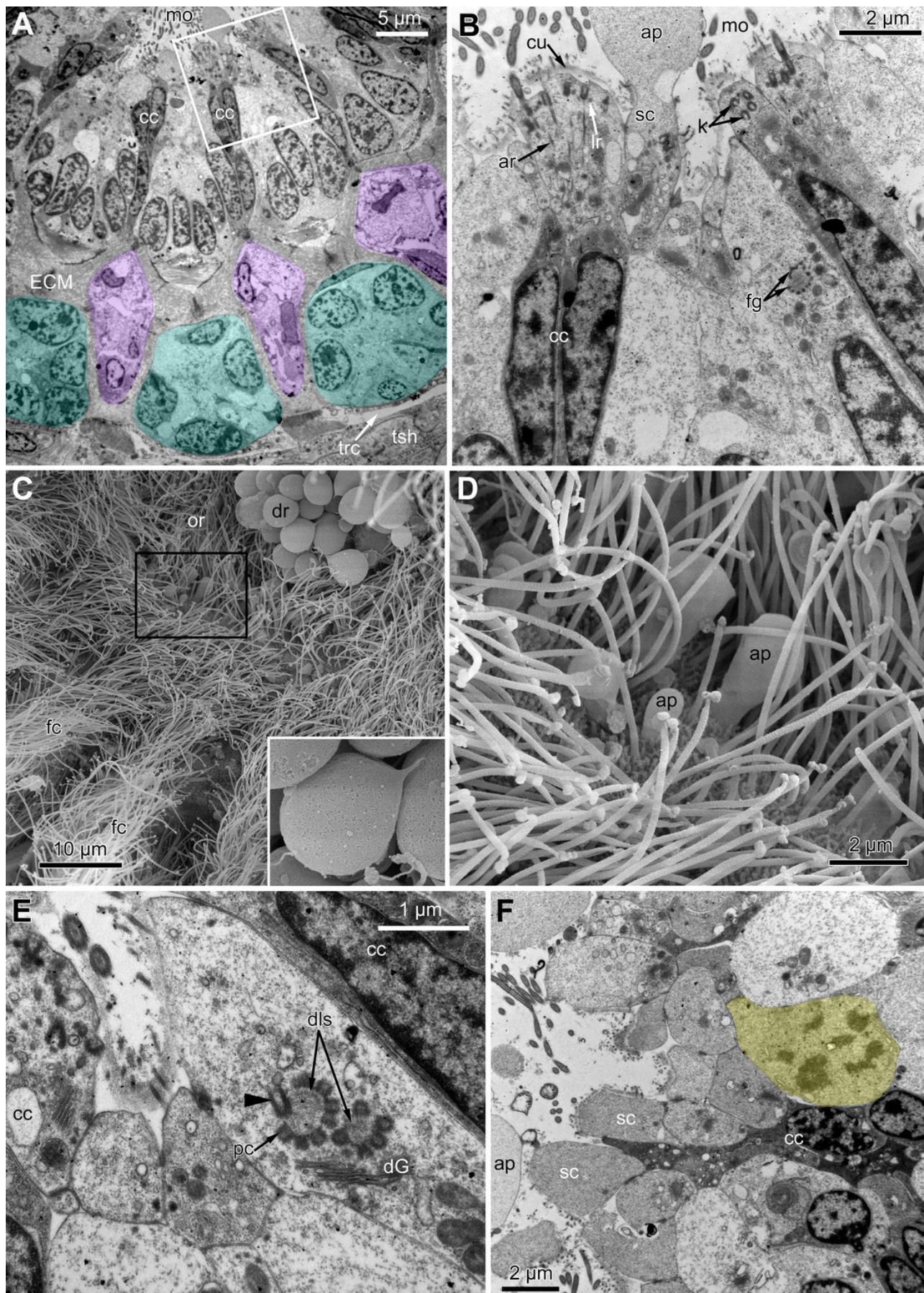
Figure 10

Figure 10: Proliferating activity in buds of *Rhamphostomella ovata* (Red – EdU-labeling, blue – Hoechst).

(A) General view of the young bud (light microscopy). (B) EdU-labeling of the young bud (CLSM, the whole mount, maximal projection). (C) General view of the late bud (light microscopy). (D) EdU-labeling of the late bud (CLSM, the whole mount, maximal projection). Abbreviations: gu – gut, tb – tentacle buds, te – tentacles.
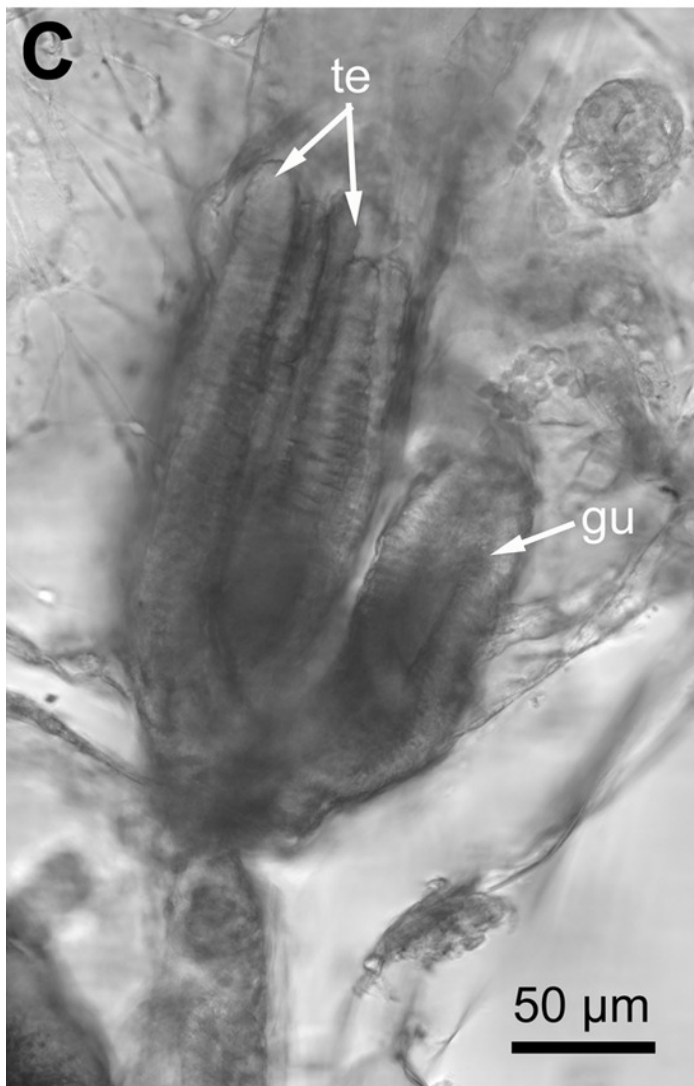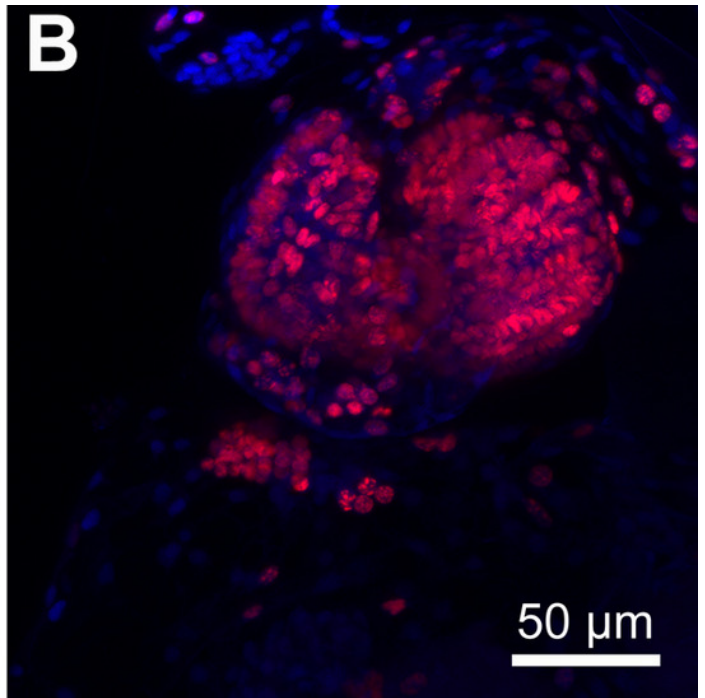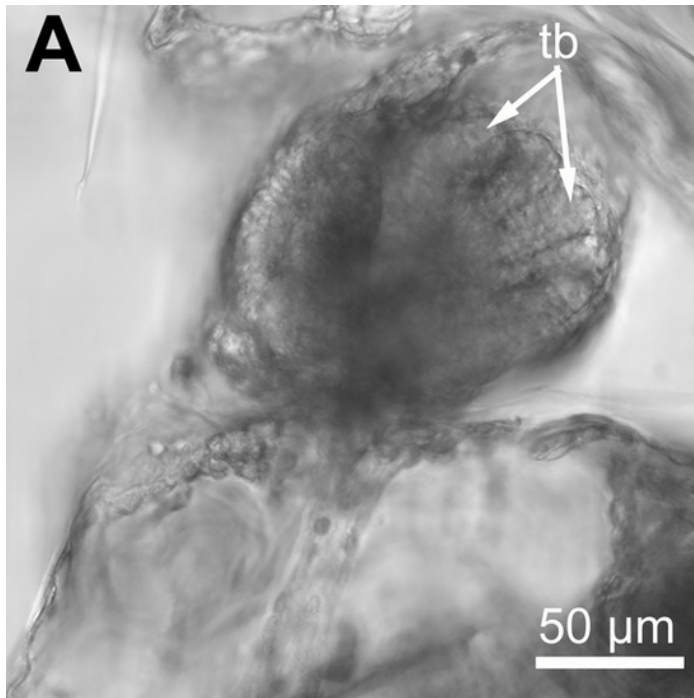
Figure 11

Figure 11: Proliferating activity in 'young' polypides (CLSM; maximal projections; Red – EdU-labeling, cyan – Hoechst).

(A) The lophophore of the young polypide (1st age class) in *Aquiloniella scabra* showing EdU-labeled cells (*arrowheads*) in the lophophore base and at the abfrontal surface of the tentacle base (whole mount). (B) The lophopore base of young polypide (1st age class) in *Rhamphostomella ovata* demonstrating EdU-labeled cells in the lophophore base (whole mount). (C) The lophophore base of the same polypide in *R. ovata*; a substack of 11 slices (from 7 to 17) showing location of DP-, EP- and P-cells within ciliated pits. (D) The lophophore base of the same polypide in *R. ovata*; a substack of 11 slices (from 7 to 17) demonstrating EdU-positive cells at the abfrontal surface of tentacle bases (*arrowhead*) and within the proximal and middle regions of ciliated pits (*double arrowhead*). (E) The lophophore base of the same polypide in *R. ovata*; a substack of 12 slices (from 27 to 38) demonstrating clusters of EdU-positive cells within the oral region (*arrowhead*). (F) The lophophore of young polypide (1st age class) in *Electra pilosa* showing individual EdU-positive cells scattered along the abfrontal surface in the proximal part of tentacles. Abbreviations: CP and DP – vertical rows of the cells composing the lateral walls of the ciliated pit and located below the corresponding C- and D-cells of the neighboring tentacles; EP – cells composing the abfrontal surface of the ciliated pit; PC – P-cells (cells located in the proximal region of the ciliated pit); cp – ciliated pit, lb – lophophore base, ph – pharynx, re – rectum, te – tentacles, tsh – tentacles sheath.
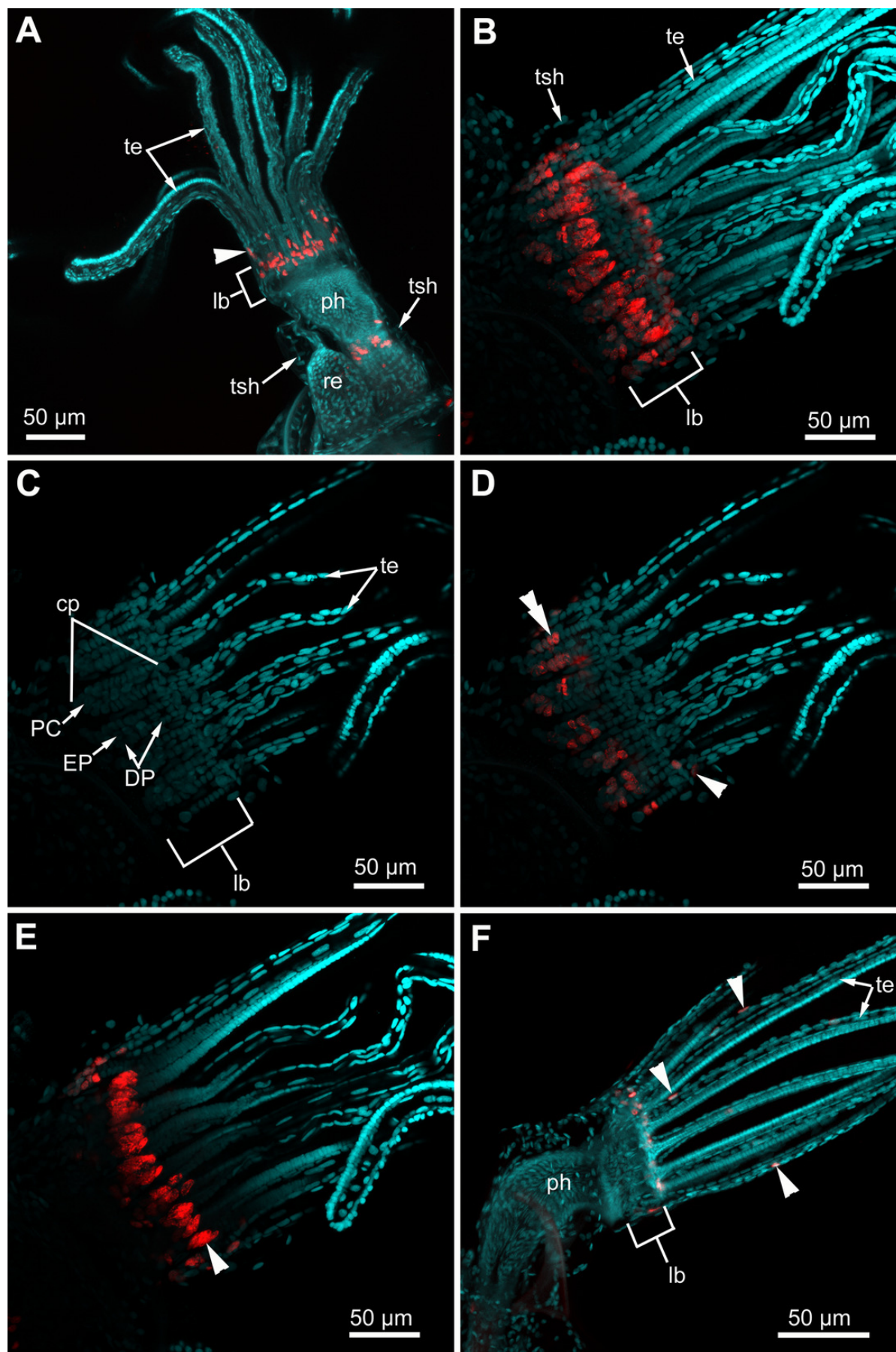
Figure 12

Figure 12: Proliferating activity in the lophophore of adult polypides (6th age class) in *Electra pilosa* during experimental tentacle regeneration.

Red – EdU-labeling, blue – Hoechst; (A–D): 48 hours after operation; (E–G): 120 hours after operation. (A) General view of the polypide with regenerating tentacles (light microscopy); 1-4 – numbered wounded tentacles. (B) Distribution of EdU-positive cells in the lophophore of the same polypide (CLSM, whole mount). Note a EdU-positive signal in E-cell (*arrowheads*) close to the wound. (C) Distribution of EdU-positive cells in the operated tentacle #2 of the same polypide (CLSM, substack of 13 slices: from 7 to 19). Note a EdU-positive signal in E-cell (*arrowhead*) close to the wound. (D) Distribution of EdU-positive cells in the operated tentacle #1 of the same polypide (CLSM, substack of 14 slices: from 32 to 45). Note a EdU-positive signal in E-cell (*arrowhead*) close to the wound healing. (E) General view of the polypide with regenerating tentacles (light microscopy). (F) The tips of regenerating tentacles of the same polypide (CLSM, substack of 28 slices: from 8 to 35). Note a EdU-positive signal in the E-cell (*arrowheads*) close to the wound. (G) The lophophore base of the same polypide showing EdU-positive cells in the ciliated pits (CLSM, maximal projection of half a polypide).
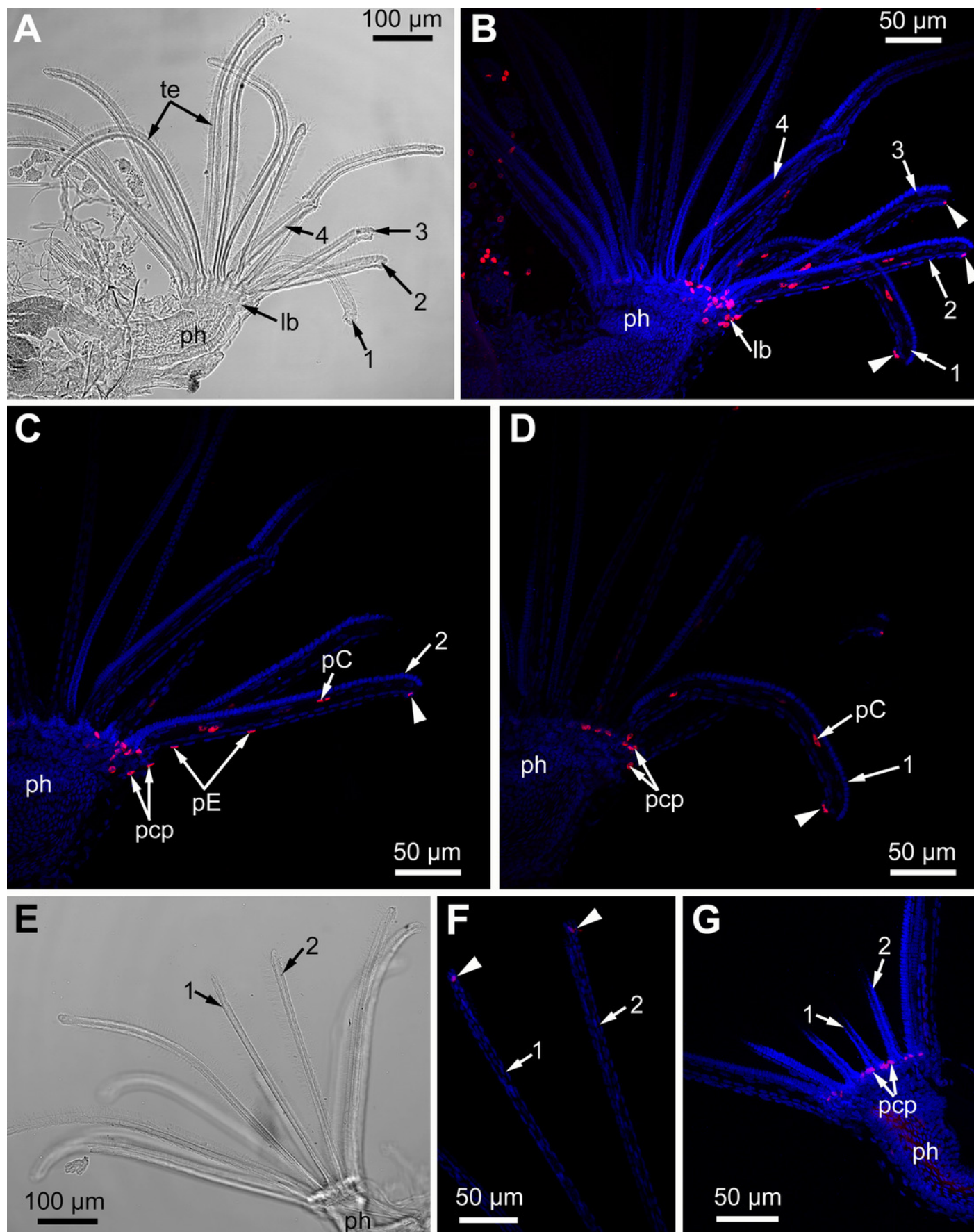
The average number of EdU-positive sells per ciliated pit in studied species.

"Young" polypides belong to the 1st and 2nd age classes, "adult" polypides belong to 4th and older age classes. SE – standard error.

1   Table 1. The average number of EdU-positive sells per ciliated pit in studied species.
2   "Young" polypides belong to the 1st and 2nd age classes, "adult" polypides belong to 4th and older
3   age classes. SE – standard error.

Species	*Rhamphostomella ovata*		*Aquiloniella scabra*		*Electra pilosa*	
Polypide age	young	adult	young	adult	young	adult
Number of studied polypides	12	9	11	8	10	14
Number of studied ciliated pits	109	99	68	67	79	134
Average number of EdU-positive cells per ciliated pit (±SE)	13.7±0.21	8.7±0.18	5.2±0.15	3.4±0.07	3.7±0.17	1.8±0.09